Structural characterization and distribution of zebrafish germ plasm during interphase and mitosis

Dissertation

**zur Erlangung des akademischen Grades
eines Doktors der Naturwissenschaften (Dr. rer. nat.)**

**im Fachbereich 18 Naturwissenschaften
der Universität Kassel**

vorgelegt von

Natalia Mackenzie Felsenhardt

Kassel, April 2007

Supervisors: Prof. Dr. Mireille Schäffer
PD. Dr. Reinhard Schuh

Committee: Prof. Dr. Mireille Schäffer
PD. Dr. Reinhard Schuh
Prof. Dr. Wolfgang Nellen
Prof. Dr. Markus Maniak

Date of Defence: 13. June. 2007

In thankful honor to my mother Krystina,
my father Kenneth, my sister Michelle and my
nephew Lucas.

Index

Abbreviations

Amp	Ampicillin
Dig	Digoxigenin
dnd	*dead end*
DynL2	Dynein light chain 2 like
dpf	day post fertilization
E.coli	*Escherichia coli*
EDTA	Ethylene diamine tetra actetic acid
g	Gravity
GFP	Green fluorescence protein
H1M	H1 type linker histone
Hpf	Hours post fertilization
Kif11	Kinesin 11
min	Minutes
ml	Milliliter
nos1	*nanos-1*
NUPL1	Nucleoporin like 1
NUP155	Nucleoporin 155
P50	Dynamitin
PBS	Phosphate buffered saline
PCR	Polymerase chain reaction
PGC	Primordial germ cell
ROI	Region of interest
rpm	Rotations per minute
RT	Room temperature
sec	Seconds
U	Units
UTR	Untranslated region
V	Volt
v	volume
wt	Wild type

1.0 Introduction

In metazoan species, sexual reproduction is accomplished through the fusion of two haploid gametes, the egg and the sperm. The differentiation of the germ cells into functional gametes and the generation of haploid genomes via meiotic cell division are critical processes in maintaining diversity and adaptability in organisms.

Germ cells, from which gametes develop, arise outside of the gonad early in development in the form of primordial germ cells (PGCs). In different organisms, PGCs form within different tissues and migrate soon after their specification towards the region where the genital ridges develop before the gonads are formed [1, 2]. Once they arrive at the genital ridges, PGCs associate with somatic gonad cells and proliferate and differentiate to generate gametes. Eventually, germ cells undergo meiosis, the germ cell-specific cell cycle. This phase of their differentiation allow for the recombination of the parental genomes as the DNA repair machinery tightly controls DNA damage and epigenetic markers are erased. Most organisms produce gametes throughout most of their adult life thanks to the presence of germline stem cells that keep producing germ cells that differentiate into gametes [3]. Although the aspects of extra-gonadal PGC formation and migration are similar in many organisms, the specific ways of how PGCs are formed early in development differ greatly within the animal kingdom. In general, there are two different ways in which PGCs are specified: either by inductive interactions between tissues or by inheritance of cytoplasmic determinants [4].

In mammals, germ cells are specified shortly before the onset of gastrulation from a group of pluripotent cells that respond to induction signals secreted by embryonic tissues [5]. In contrast, in other organisms including zebrafish, *Xenopus*, *Drosophila* and *C.elegans*, the specification of the germ cell linage occurs earlier in development, and is dependent on the asymmetrical distribution of specialized cytoplasmic material originally deposited in the oocyte, denominated germ plasm [6].

1.1 Germ cell specification and germ plasm

As previously mentioned, in animals like zebrafish, *C. elegans* and *Drosophila* germ cell specification occurs upon asymmetrical distribution of the determinants collectively termed germ plasm. [7, 8]. This special type of cytoplasm is composed by maternally provided RNAs and proteins, which are transported from the yolk to the developing embryo after activation upon fertilization.

In organisms like *C. elegans*, *Drosophila* and zebrafish the germ plasm is an electron-dense material that is associated with fibrils, mitochondria and the nuclear envelope, commonly known as nuage because of its cloudy ultrastructual appearance.

In *Drosophila*, nuage is the precursor of the polar granules and is first detected in nurse cells [9, 10]. During oogenesis, these polar granules are recruited and assembled in the posterior pole of the oocyte. During early embryogenesis cells located at the posterior part of the embryo incorporate the germ plasm and assume the germ cell fate (pole cells) [11]. Once the pole cells are formed, the granules associate with the outer nuclear envelope, remaining in the germ cells though out the life cycle of the *Drosophila.*

Similarly, the segregation of the germ cell linage in *C.elegans* occurs early during embryonic development, where the primordial germ cell P4, is generated via a series of unequal divisions. These divisions produce the germline blastomeres denominated P (1), P (2), P (3) and P (4) that differ from somatic cells in their size, fate and germ plasm content [12].

In zebrafish, germ plasm is localized to the furrows of the first and second cleavage divisions of a newly fertilized egg, and after consecutive divisions is incorporated into four different cells that will become the germ cell lineage progenitors [13]. Importantly, it has been shown that if the germ plasm is eliminated from the cleavage furrows, germ cell determination in zebrafish is defective [14]. Similarly, experiments in Drosophila [15] demonstrated that nuage miss-localization by transplantation gives rise to ectopic germ cell clusters. Additionally, studies in zebrafish revealed that components of the germ plasm

such as the RNA-binding protein Dead End 1 (Dnd1) and Nanos1 (Nos1) are essential for germ cell survival [16, 17]; Dead-End and Nanos deficient germ cells die after specification.
Hence, germ plasm is essential and sufficient for specification and survival of germ cells in the early stages of development.

1.2 Germ plasm components

Several components of the germ plasm have been identified, appearing to be highly conserved within the animal kingdom. One characteristic component of the germ plasm is the *vasa* gene, originally identified in *Drosophila* as a maternal gene required for the formation of the abdominal segments and germ cell specification [18]. Vasa belongs to the family of RNA helicases, constituted by a large group of conserved enzymes that use ATP hyrdolysis to modulate the RNA structure. RNA helicases are mostly involved in transcription, splicing and translational regulation. Through their ability to modulate RNA structures they can regulate protein expression, and therefore, cell differentiation [19]. In *Drosophila*, Vasa was described to be involved in germline cyst growth, oocyte differentiation, egg chamber patterning [20], and normal development of PGCs [21, 22]. Interestingly, Vasa protein was first described to be similar to the eIF-4A eukaryotic initiation factor [21], which plays an essential role in unwinding RNA secondary structures allowing ribosomal attachment and translation. In *Drosophila,* Vasa was also described to regulate translation of germline specific germ plasm components like Nanos, a protein involved in normal body plan [23] and germ cell development in several organisms including zebrafish [17]. Interestingly, in planarians, somatic cells identified as neoblasts, a totipotent cell type that functions in regeneration, also expressed a *vasa* homolog [24]. Hence, Vasa protein may function in the preservation of germ cell totipotency by mechanisms such as inhibition of genes that lead to somatic differentiation.
In zebrafish, maternal *vasa* RNA is localized to the cortex of oocytes and upon fertilization, it concentrates at the base of the blastodisc between the yolk and cytoplasm of one-cell embryos [25]. *Vasa* RNA subsequently becomes enriched

at the distal ends of the cleavage furrows in 2-cell and 4-cell embryos, first as rod-like structures and subsequently as compact aggregates at the periphery of the furrow [26, 27] reviewed in [28] (Fig.1). This localization process is dependent on actin and microtubules rearrangement [27, 29]. At the 32-cell stage, these RNA aggregates ingress into four cells, the progenitors of the germ cells, and segregate asymmetrically during cell division. Therefore, only one daughter cell inherits the germ plasm until sphere stage (Fig.1g insert) [13, 30]. While somatic cells increase dramatically in numbers, asymmetric segregation of the germ plasm generates a constant number of presumptive germ cells. From late blastula on (4 hours post fertilization (hpf)), *vasa* mRNA segregation changes from asymmetric to a symmetric localization, an event that precedes primordial germ cell proliferation (Fig.1h insert). At this time, Vasa protein appears for the first time to colocalize specifically to PGC, adopting perinuclear localization [13] while during early stages it is expressed in all blastomeres. This change in localization pattern in PGCs does not depend on zygotic gene expression, although it coincides with zygotic *vasa* transcription and an increase of Vasa protein levels [13]. Additionally, translation of maternal RNA provides a minor contribution to the localized Vasa protein in PGCs, whereas protein accumulation relies more on translation of zygotically expressed *vasa* RNA [13]. It is believed that maternally localized *vasa* mRNA may promote an initial enrichment of Vasa protein in PGCs. Maternally derived Vasa protein could then initiate, possibly by translational activation of specific transcripts, zygotic *vasa* gene expression and therefore germ cell specification [28]. Therefore, it is tempting to speculate that localization of *vasa* RNA to the germ plasm may be done in order to restrict Vasa protein expression to the future PGCs.

As previously mentioned, another germ plasm component is *nanos* RNA, which encodes an RNA binding zinc finger protein. Although is not required for PGC formation, Nanos-deficient PGCs develop abnormally. They fail to incorporate into the gonad, show premature activation of germ cell markers, exhibit abnormal morphology, and express mRNAs that are normally present in the soma [31, 32]. In different organisms including zebrafish and *Drosophila*, there is a conserved

mechanism that restricts Nanos protein to the PGCs during embryogenesis [17, 33] [34]. This mechanism ensures poor translation and active degradation of *nanos* mRNA in somatic cells, but specific mRNA protection from those processes in PGCs by sequences residing in the 3' untranslated region (3'UTR). This asymmetric RNA localization and the differential translation and degradation properties of the RNA result in specific expression of Nanos in PGCs, leading to proper germ cell differentiation. Interestingly, it has been recently shown that micro RNAs are involved regulating the differential translation of *nanos* RNA, allowing specific expression of the protein in the germ cells [35].

Due to the PGC-specific mRNA stabilization of the *nanos* mRNA 3'UTR, zebrafish *nanos* UTR is widely used for directed expression of different genes in PGCs including fluorescent proteins [17].

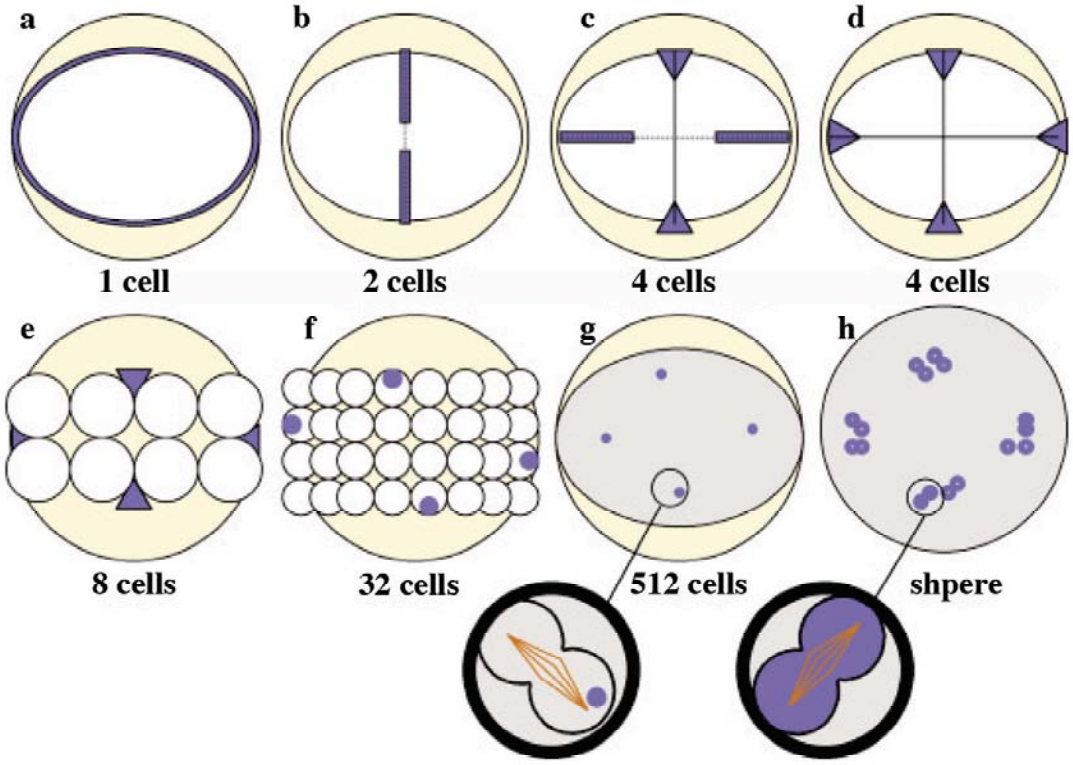

Figure 1. Segregation of maternally derived *vasa* mRNA during early embryogenesis (see next page)

Cartoon of an animal view of zebrafish embryos. a) *Vasa* mRNA becomes localized to the cytokinetic ring during egg activation upon fertilization. b,c,d,e) At the first and second cleavage the RNA is recruited to the forming furrows and forms tight aggregates upon furrow maturation, a process that is dependent on microtubules. f) At 32-cell stage aggregates ingress into four cells, where they remain localized and segregate asymmetrically during cell division (g and insert). h) At sphere stage (4hpf) *vasa* mRNA becomes evenly distributed within cells and segregates symmetrically during cell division (insert h). Brown structures in the inserts represent microtubules of the spindle apparatus, whereas purple depict germ plasm. (Adapted from [28])

1.3 Germ plasm segregation in later stages of development

After 4 hours of zebrafish development, conglomerates of germ plasm proteins localize around the primordial germ cell nucleus, forming spherical structures known as perinuclear granules or germinal granules. This reorganization around the germ cell nucleus ensures that as division proceeds, both daughter cells will receive germ plasm and therefore, the number of PGCs increases [36].

Germinal granules have been described in many species as RNA-protein complexes, a possible storage of RNA and proteins involved in transcriptional and translational regulation [30]. Although a detailed description of their function is still necessary, its components are involved in regulation of maternal mRNA expression. Genes involved in proper structural maintenance of granules have been demonstrated to be essential for germ cell survival and development. One example is the *tudor* gene, initially described in *Drosophila* to be necessary during oogenesis for determination and formation of primordial germ cells, and for abdominal development [37]. Studies revealed that Tudor proteins act as essential scaffolds for proper germ plasm assembly: without proper Tudor function, granule structure is altered and germ cells are not formed [38].

Although a detailed description of germ plasm distribution has been made in early stages of zebrafish development [13], little is known about the distribution of the material during mitosis after germinal granules adopt perinuclear localization. Moreover, it is not clear whether there is a controlled mechanism that ensures

the deposition of germ plasm in both daughter cells after cell division, allowing maintenance of germ cell fate during later stages of development.

1.4 Cell cycle and germ plasm segregation during mitosis

It is likely that major players involved in cell cycle are involved in germ plasm segregation in primordial germ cells. Therefore, we will describe the function of several cellular components during interphase, and the transformations that they undergo during mitosis.

Cell cycle is the series of events in a eukaryotic cell between one cell division and the next, which consists of four distinct phases: the G1 phase, S phase, G2 phase (collectively known as interphase), and the mitotic phase.

Mitosis is the process by which eukaryotic cells separate its duplicated genome into two identical halves. Followed immediately by cytokinesis, the cytoplasm and cell membrane are divided, resulting in two genetically identical daughter cells with a roughly equal distribution of organelles and other cellular components [39] [40]. This fundamental mechanism is dependent on the activation of the mitotic spindle, a molecular machine assembled by microtubules (MTs) and motor proteins [39] [41].

1.4.1 Microtubules (MTs)

Microtubules are involved in many cellular processes during the entire cell cycle, including transport of proteins and organelles, establishment of cell polarity, and formation of the meiotic and mitotic spindle.

During mitosis, microtubules form the spindle apparatus, which consists of two poles in which the MT minus ends are nucleated and anchored to the centrosomes, whereas the plus ends extend outwards connecting to the kinetochores of each chromosome, or to the plasma membrane (Fig. 2). During the cell cycle, the mitotic spindle is assembled in a temporally regulated manner, and the organization of the MTs and the movement of chromosomes, while being segregated to the daughter cells, are achieved through a complex set of forces.

These forces are in part dependent on MTs instability, characterized by switching between periods of growth and shortening, driven by polymerization and depolymerization of Tubulin in the plus ends. These changes in polymerization exert forces including chromosome capture [42] [43], and chromosome movement mediated by kinetochores [44]. In addition to microtubule dynamics, forces exerted by both plus and minus end directed motors are required for normal assembly of the mitotic spindle.

Figure 2. The mitotic apparatus during prometaphase

Immunostaining of a human A549 cell. Microtubules (MT) originate at each of two centrosomes/spindle poles (P) and are organized in a bipolar shape. The plus ends of microtubules attach to the kinetochores (K) on each chromosome pair (C). Scale bar is 10µm. (Adapted from [45]

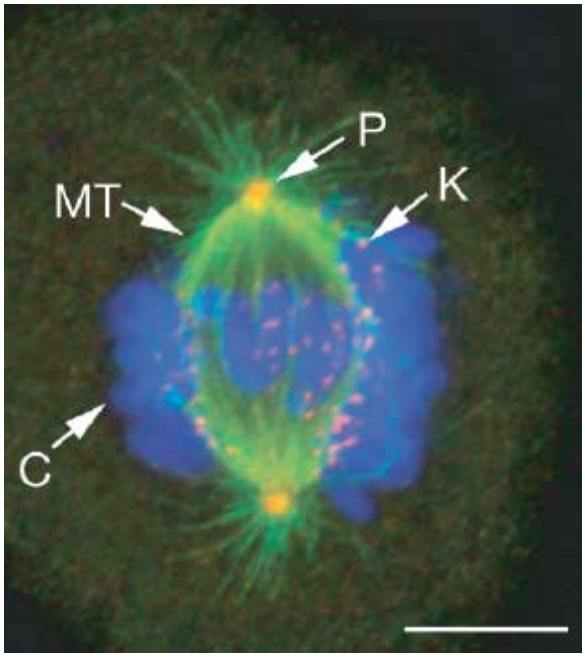

1.4.2 Molecular motors

Molecular motors are proteins that convert chemical energy to mechanical work and motion. Additionally to participating in the formation of the mitotic spindle, motor proteins such as Kinesin and Dynein play a crucial role in translocation, tension and organization of cellular components during the cell cycle [46].

Kinesins are processive plus-end directed motors that move unidirectionally along linear tracks of microtubules (Fig. 3a). Members of the Kinesin family have been implicated in vesicle and organelle transport, spindle and chromosome

motility during meiosis and mitosis, microtubule stabilization and flagelar and ciliary function. The Kinesin motor proteins (Fig. 3b) consist of a highly conserved motor or catalytic domain with sites for microtubule and ATP binding, joined to a α-helical colied-coil stalk [47].

Similarly but complementary, the multisubunit Cytoplasmic Dyenin is a minus end-directed motor protein complex (Fig. 3a). It also travels along microtubules, and it has been implicated in a wide variety of cellular processes [48] including mitosis, maintenance of the Golgi apparatus and trafficking of membranous vesicles and RNA particles [49, 50]. Each Cytoplasmic Dynein contains two enzymatically active heads or heavy chains (HC), which convert the energy of ATP hydrolysis into mechanical work [41]. The two globular Dynein heads are connected by slender stalks to a common base [51, 52], which consist of intermediate and light chains (Fig. 3c). The base of Cytoplasmic Dynein is thought to anchor the molecule to organelles and possibly, to kinetochores, while the globular heads interact in an ATP-dependent manner with the microtubules of the cytoskeleton [52]. For proper activity, Cytoplasmic Dynein requires another multisubunit protein complex known as Dynactin [53, 54], which acts as an adaptor protein involved in the dynein-cargo interaction [55]. Dynein action can be inhibited by over expression of the Dynactin subunit Dynamitin (p50), which destroys Dynactin function by releasing its Dynein-binding subunit [56]. During cell division, the action of Dynein motors lead to the formation of MT asters when complemented with the Nuclear Mitotic Apparatus protein (NuMA), which cross links the minus ends of MTs [57, 58]. Dynein has also been described to crosslink and slide astral MTs in relation to an actin matrix in the cell cortex, pulling the spindle poles apart and positioning the entire spindle within the cell. Additionally, Dyneins act to exert forces that push apart the spindle poles, allowing separation of daughter cells after cytokinesis [59].

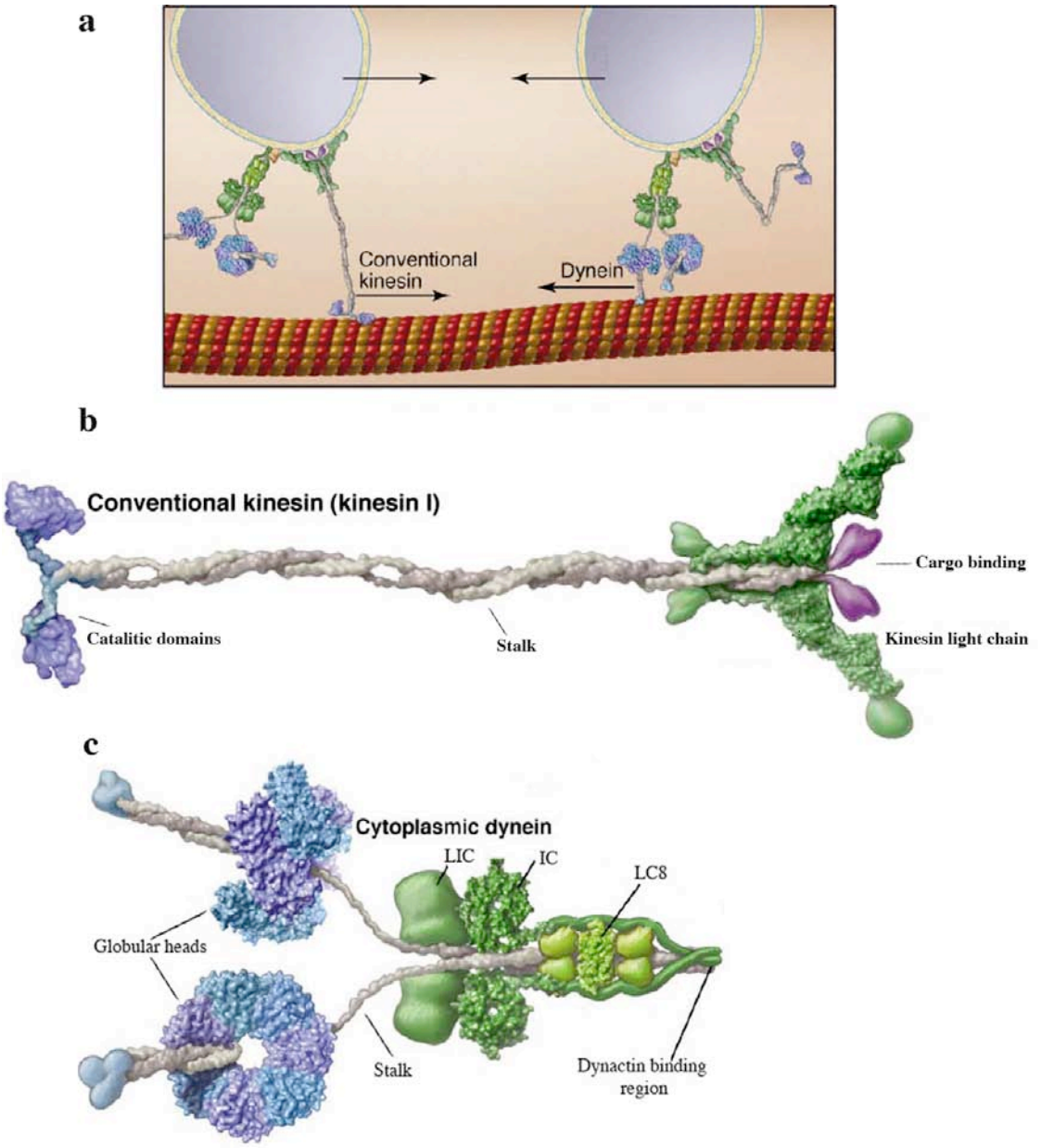

Figure 3. The molecular motors Kinesin and Dynein
a) Representation of Kinesin and Dynein motors transport of membrane organelles along an array of microtubule towards the plus end (Kinesin) and minus end (Dynein).
b) Detail of plus end-directed motor Convensional Kinesin structure. Cargo binding area is depicted in purple and is located in between the Kinesin light chains. This area is connected to the catalitic domains by a stalk.
c) Detail of minus-end directed motor Dynein structure. Two globular head domains connect by a stalk to a body composed of light intermediate chains (LIC), intermediate chains (IC) and light chains (LC8). Dynactin binding regions appear towards the cargo binding area, opposite from the motor heads. Adapted from [60].

1.4.3 The nuclear envelope

Specific localization of germ plasm to the nuclear envelope in later stages of development has been described to be one of the major characteristics of germinal granules. In order to understand the transformation that the nuclear envelope undergoes during cell division, we will briefly describe some of the nuclear envelope components during interphase.

The nuclear envelope consists of three distinct membrane domains: the outer membrane that is continuous with the endoplasmic reticulum, the inner membrane that is associated with a nuclear lamina, and the pore membrane that forms between the junction of the outer and inner membrane and is associated with the nuclear pore complexes (NPCs) [61].

1.4.3.1 The nuclear lamina

One essential nuclear envelope structure is the lamina, which is located between the inner membrane and the chromatin. This structure consists of a fibrous meshwork of type V intermediate filament proteins called lamins, which are grouped into A\C and B types on the basis of their biochemical properties [62]. Lamins are important for nuclear functions, including nuclear envelope assembly [63], nuclear size and shape, DNA replication [64], and RNA polymerase II–driven gene expression [65]. They also provide mechanical support for the structural integrity of the nucleus and anchorage sites for interphase chromatin [66].

1.4.3.2 Nuclear pore complexes (NPCs)

The transport of molecules between the cytoplasm and the nucleus is necessary for proper exchange of information within the eukaryotic cell. NPCs are formed by approximately 30 Nucleoporins (NUPs) that are in charge of exchanging ions and small molecules between the cytoplasm and the nucleus [67]. Active nuclear transport through nuclear pore complexes is a highly rapid and efficient process, where NUPs orchestrate multiple transport events at the same time [68].

Interestingly, it was demonstrated that although the NPC are associated to the nuclear membrane, they do not require the membrane either for attachment to the nucleus or for maintenance of its own structural integrity [69].
One essential molecule that shuttles from the nucleus to cytoplasm through the NPCs is mRNA. During interphase, newly transcribed mRNA associates with nuclear proteins to complexes known as messenger ribonucleoprotein particles (mRNPs), which functions vary from RNA processing to nuclear export [70]. Completion of pre-mRNA processing generates export-competent mRNPs, that efficient translocate through NPCs into the cytoplasm. However, newly exported mRNPs are not structured for proper translation, and therefore certain RNA helicases are required to unwind short double-stranded regions of RNA or to dissociate bound proteins from RNA in order to allow translation [71].

1.4.3.3 The nuclear envelope break down (NEBD) during mitosis

During cell division, the nuclear envelope of metazoans is disassembled in order to allow the establishment of a mitotic spindle apparatus that captures and segregates the duplicated chromosomes. During prophase and metaphase, the nuclear membranes either vesiculate [72, 73], fold and invaginate at the centrosomes [74], or associate to the endoplasmic reticulum (ER) [75, 76]; while many peripheral proteins associated with the nuclear membranes become dissociated and disperse in the cytoplasm. As the lamin protein interactions are weakened through phosphorylation by mitotic kinases, loss of interaction between integral proteins of the inner nuclear membrane (LAPs) and chromatin induces lamina matrix reversible disassembly. [77, 78]. Lamin dimers are removed by molecular motors and transiently accumulate near the centrosomes (Fig.4).
As mentioned before, the nuclear pore complexes are associated with the outer and inner nuclear envelope. During cell division while the nuclear envelope breaks up, some NPCs partially disassemble upon phosphorylation of their individual components [79, 80] and disperse into the cytoplasm. Others leave the nuclear envelope early in mitosis and become associated with kinetochores

where they play an essential role in microtubule-kinetochore association [81].

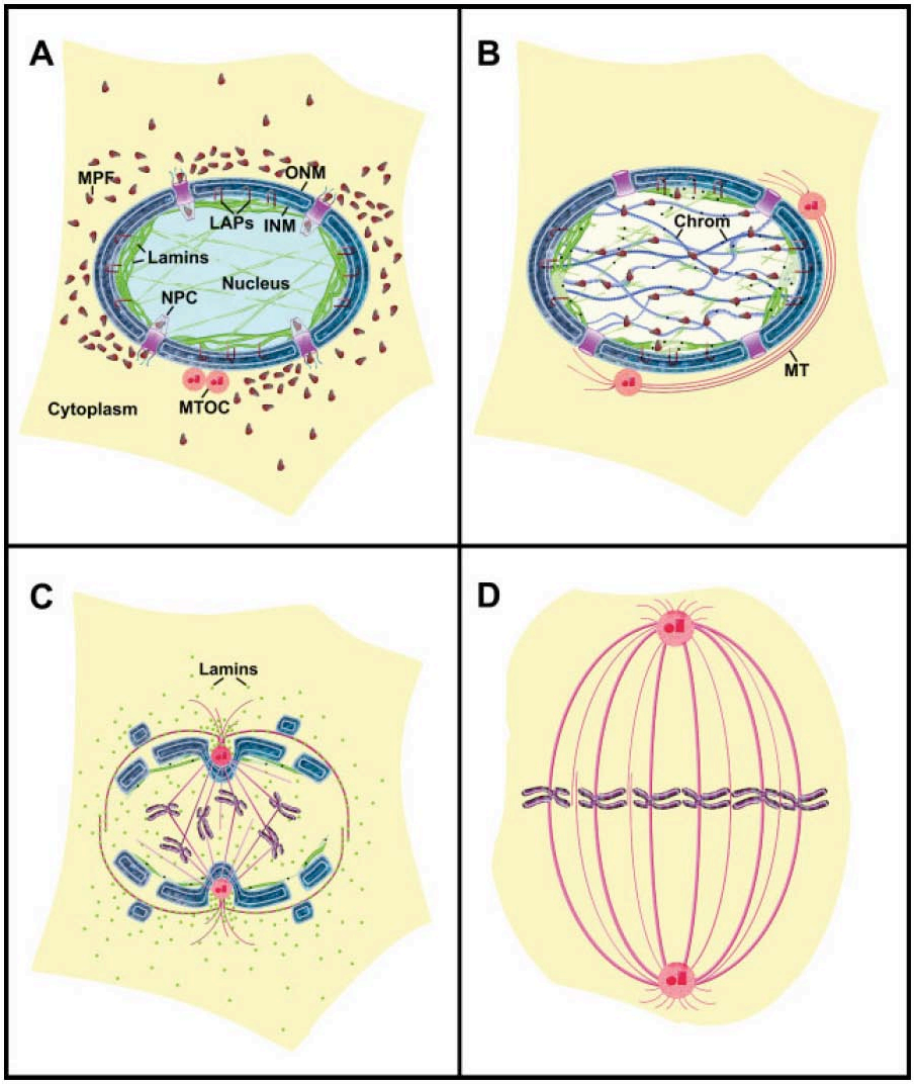

Figure 4. Model of nuclear envelope disassembly during mitosis
a) During late G2, a cyclin-dependent kinase (meiosis promoting factor, MPF) enters the nucleus through the nuclear pores and phosphorylates the target proteins. b) During early prophase, phosphorylation by MPF causes chromosome condensation, weakening of the nuclear lamina by partial disassembly of lamin filaments (light green), loss of interaction between integral proteins of the inner nuclear membrane (LAPs) and chromatin, and NPC disassembly. Centrosomes (MTOC) migrate along the outer nuclear membrane (ONM). c) At late prophase/prometaphase, chromosomes further condense and the nuclear membranes fold and invaginate at the centrosomes. NPCs are probably completely disassembled and lamin dimers are removed by molecular motors and transiently accumulate near the centrosomes. d) During metaphase, the chromosomes are aligned in the mid-plane and the nuclear envelope is completely disassembled. (Adapted from [74])

1.4.3.4 The nuclear envelope reassembly during mitosis

As mitosis nears completion, the preexisting pools of nuclear envelope precursors are used in the process of nuclear envelope re-assembly. Membrane vesicles bind to the surface of daughter chromosomes and fuse into flat cisternae [82], a process that begins during anaphase. The emerging consensus is that inner-membrane proteins mediate membrane attachment. Thus, increasing availability of chromatin and lamin binding sites leads to the immobilization of more inner-nuclear membrane proteins. After the formation of a continuous double membrane around the chromosomes, the first event of pore complex reassembly occurs when a nucleoporin complex localized to both sites of the central core of NPCs binds chromatin [74, 83]. At the same time, lamins are either recruited to chromosomes, or transported into the nucleus through NPCs followed by repolymerization of the nuclear lamina. More specifically, while B-type lamins are detected at chromosomes at early stages of nuclear envelope reformation, lamin A\C-type translocate through the newly formed NPCs and redistributes in the nuclear interior during telophase/G1 [74].

1.4.4 Distribution of cytoplasmic components during cell division

The requirement of accurate inheritance of organelles and cytoplasmic components is a main event during cell division. Once the genetic material is duplicated, there is a reorganization of the cytoskeleton to form the spindle that mediates the segregation of the duplicated centrosomes to opposite poles. After DNA condensation and nuclear envelope disassembly, the spindle microtubules attach to kinetochores of individual sister chromatids, pulling them towards the area where the nucleus will form in the respective daughter cells [40]. Without proper regulation of chromosome distribution, genomic stability is seriously altered, where abnormal distribution of chromosome may cause tumors and genetic diseases [40, 84]. Accuracy in organelle inheritance is as well an essential requirement for cell survival. ER needs to be inherited since the synthesis of all membranes linked by vesicle–mediated transport including Golgi

apparatus, lysosomes, endosomes, plasma membrane and secretory granules, originate in large part from proteins and lipids originated in the ER [85]. Mitochondria and chloroplasts also need to be properly segregated as they carry their own essential DNA and tRNAs and are not synthesized *de novo* [86]. As for genetic material, organelle inheritance proceeds by growth, replication and partitioning phases. Once an organelle is doubled in biomass in preparation for cell division, it must be accurately partitioned between progeny. Organelles adopt one of two different partitioning strategies: ordered or stochastic [87]. Ordered partition often involves the mitotic spindle and is associated to microtubules, having the distribution of sister chromatids into the forming daughter cells as the most representative example. Contrarily, a stochastic mechanism relies on random probabilities of distribution that may be analyzed statistically, but may not be predicted precisely. In other words, stochastic partitioning relies on a randomness of multiple organelle copies within the cell that would provide each daughter cell with sufficient copies of the organelle, but not necessarily the with the same total number. Depending on the organelle, stochastic distribution may exhibit a tendency towards equality [87]. For example, the large cytoplasmic area covered by the ER in mammalian cells ensures that by a stochastic mechanism, both daughter cells inherit enough amount of ER [88].

Even if a daughter cell is able to synthesize an organelle *de novo* this process is extremely slow, generating a strong selective disadvantage [89]. Ordered and stochastic strategies are not mutually exclusive, and which one is used depends on organelle copy, cell type and type of organism [88]. Interestingly, both mechanisms may operate together [90], especially when the number of organelles that need to be distributed is low. A complete random distribution where components are lost by one of the daughter cells during cell division has not yet been described.

1.4.4.1 Germ plasm distribution in mitotic germ cells

Due to the essential role the components of the perinuclear granules play in germ cell development, it is crucial to ensure a proper distribution of the material

between both daughter cells in order to guarantee the endurance of the germ cell linage. However, the mechanism that segregates these structures during cell division during the first 24 hours of embryonic development is unknown.

1.5 Aim of the thesis

The focus of this thesis is the structural characterization of germ plasm material in zebrafish primordial germ cells between 4hpf and 24hpf of embryonic development. In addition, the mechanisms controlling germ plasm distribution within the cell throughout the cell cycle where examined.

2.0 Results

At the 32-cell stage of zebrafish embryogenesis, 4 blastomeres become the progenitors of all germ cells as they integrate the germ plasm. During mitosis, this material localizes to one spindle pole, being distributed asymmetrically into the daughter cells, therefore limiting the number of germ cells during this first stage of proliferation. At approximately four hours post fertilization (hpf), proteins of the germ plasm localize around the germ cell nucleus, forming sphere-like structures known as perinuclear or germinal granules. This reorganization around the germ cell nucleus coincides with an increase in PGCs number, and it is believed that this reorganization ensures the even distribution of material among daughter cells as division proceeds [36]. However, whether this segregation into daughter cells is done by a controlled mechanism remains unknown.
We hypothesize that since germ plasm is critical for proper germ cell development, the distribution of germinal granules is a regulated process. We further assume, that similar to the control of germ plasm distribution in early stages of development, cytoskeletal components may play a role in granule segregation during mitosis after 4 hours post fertilization (hpf).

In order to visualize the different steps of cell division and granule distribution by fluorescence microscopy, genes coding for components of the nuclear envelope, microtubules, molecular motors and germinal granules were cloned and fused to GFP or DsRed fluorophores. Germ cell-specific labeling was achieved by injection of RNA into one cell stage zebrafish embryos. All gene fusions were under the control of the *nanos* 3'UTR in order to specifically direct expression to PGCs.
To verify that all genes used in this work are expressed by germ cells, RNA *in situ* hybridization was performed for genes whose RNA expression has not been previously described. The expression patterns of the nuclear pore component *nucleoporin 155* (*NUP155*), and the molecular motors *dynein light chain2 like* and *kinesin11* RNAs were previously described in the zebrafish database

(www.zfin.org). The three genes appeared to be ubiquitously expressed from 0 to 60 hpf in the case of *NUP155* and *dynein light chain2 like*, and from 6hpf to 24hpf of zebrafish development in the case of *kinesin11*. In the case of the nuclear envelope genes *lamin B2* and *nucleoporin L1* (also known as *NUPL1*) RNA *in situ* hybridization indicates ubiquitous gene expression in zebrafish embryos during the first day of development (Fig. 5). This suggests that PGCs express all genes used in this work during all stages that were analyzed.

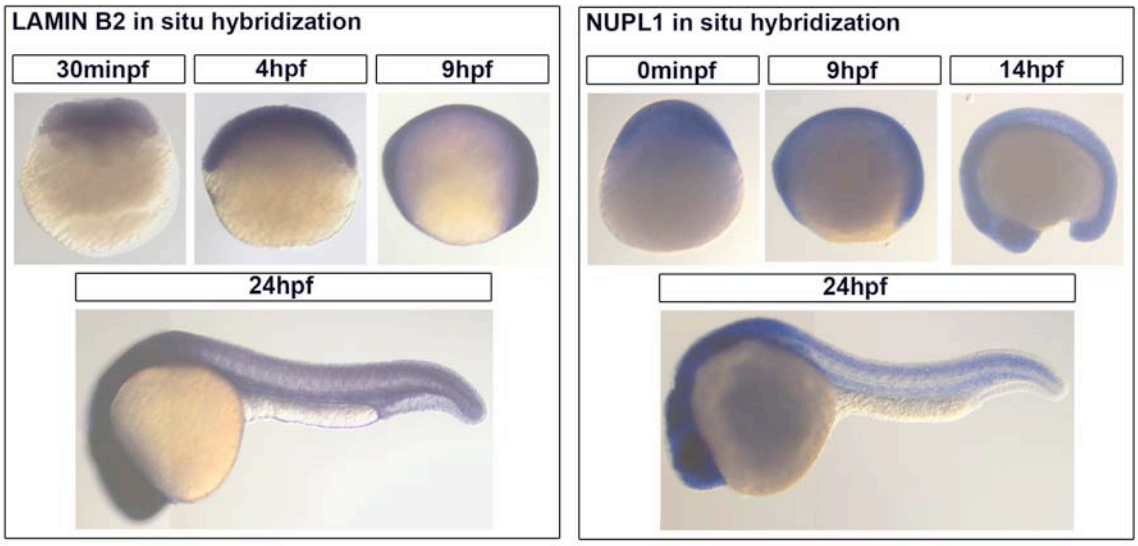

Figure 5. L*amin B2* and *nucleoporin L1* are ubiquitously expressed during the first day of zebrafish development
RNA expression of the nuclear envelope l*amin B2* and *nucleoporin L1* was detected by *in situ* hybridization. Both *lamin B2* and *nucleoporin L1* RNAs are ubiquitously expressed in embryos from 30 minutes post fertilization to 24hpf in the case of *lamin B2* and from 0hpf to 24hpf in the case of *nucleoporin L1*.

2.1 Localization and distribution of perinuclear granules during cell division

To elucidate how perinuclear granules are distributed among daughter cells during mitosis, we analyzed germ cell division in 10hpf zebrafish embryos, and followed distribution of germinal granules. RNAs of v*asa-DsRed-nos1*-3'UTR,

laminB2-GFP- nos1-3'UTR and *NUPL1-gfp- nos1-3'UTR* were injected into one cell stage zebrafish embryos in order to label perinuclear granules and nuclear envelope respectively. Nuclear envelope break down (NEBD) and granule segregation during cell division were observed using confocal time-lapse microscopy.

At 10hpf, perinuclear granules of diverse sizes are organized around the nuclear envelope of interphase germ cells (Fig. 6a, movie 1). At the onset of cell division during early prophase, the nuclear envelope disassembles and perinuclear granules lose their localization and randomly spread throughout the cell during metaphase (Fig. 6a). As this scattering of granules takes place, they maintain their spherical morphology (observation is based on the size of the protein complex visualized using the molecular marker Vasa). Transiently, granules may change their shape following structural alterations of the envelope during nuclear disassembly in early prophase, recovering their spherical shape when detached completely from the envelope during metaphase (Fig. 6a, early prophase, arrow).

At the end of cytokinesis the nuclear envelope re-assembles as visualized by the reformation of the Lamin B2 network (Fig. 6b, movie 2). At this time, several granules are already located in the area where the nuclear envelope is forming, while those located in the cytosol far from the nucleus collectively move directly towards the forming nuclear envelope. Granules re-associate with the envelope within approximately 6.8 minutes. To confirm this observation, we labeled the nuclear envelope with the nuclear pore complex component NUP155 fused to GFP (Fig. 6c, movie 3). As in LaminB2-GFP labeled germ cells, direct movement of perinuclear granules towards the area where the nuclear envelope reassembles accompanies the termination of mitosis. The latter time-lapse revealed a faster re-localization of granules of approximately 3 minutes, where the total time for mitosis in germ cell is approximately 14 minutes.

These results suggest that the perinuclear localization of granules, but not their spherical shape, is dependent on the nuclear envelope integrity. Moreover, during nuclear envelope re-assembly all granules readopt perinuclear localization

within approximately 3 to 6.8 minutes after mitosis with no evident morphological alteration.

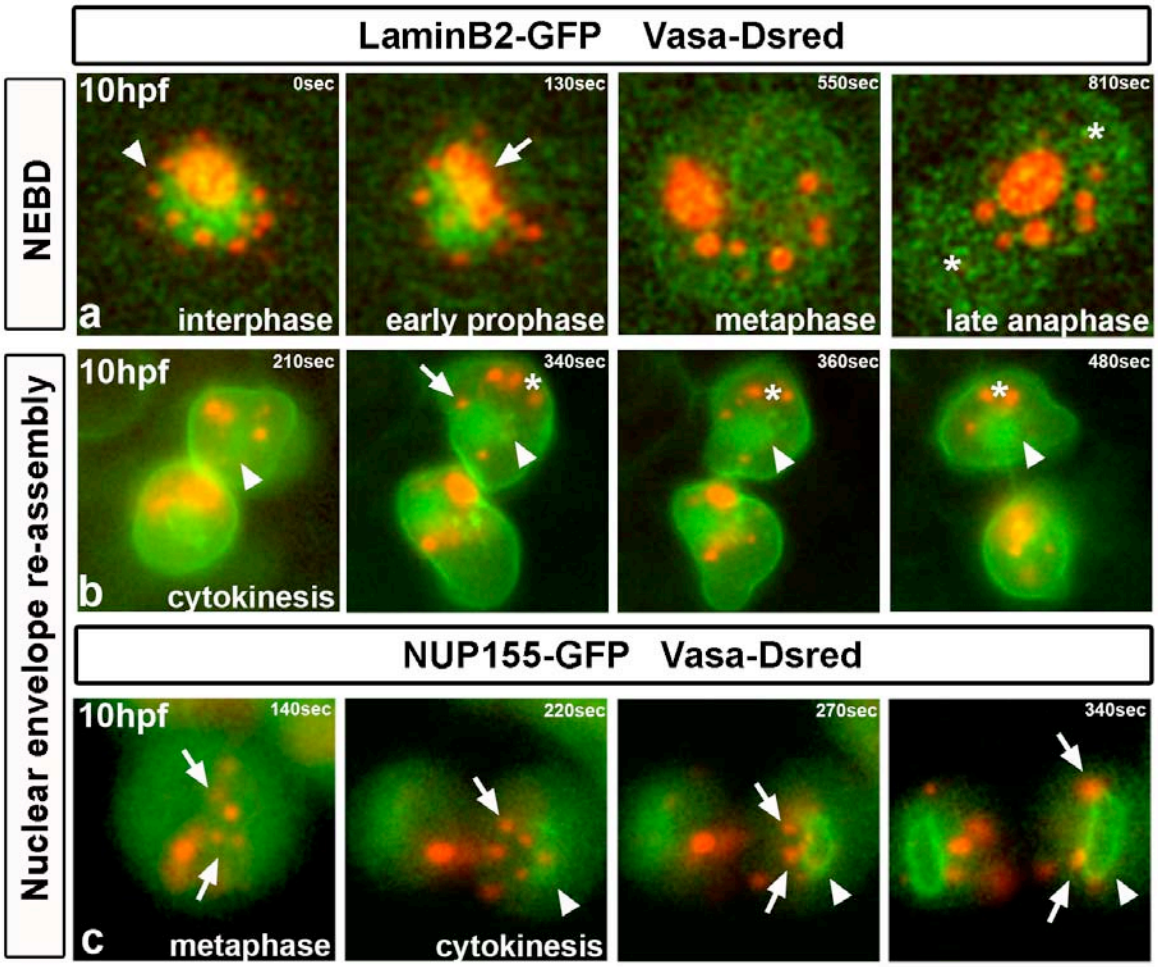

Figure 6. ***In vivo*** **perinuclear granule behavior during cell division**
a) Granules are visualized by Vasa-DsRed expression and nuclear envelope by LaminB2-GFP. Time is specified for each frame in upper right corner. During interphase and before nuclear envelope breakdown (NEBD), granules (arrowhead) show an organized localization around the nucleus labeled in green. During early prophase, the nuclear envelop starts to disassemble and germinal granules change their shape following the nuclear envelope rearrangement (arrow). Once the envelope is completely disassembled during metaphase, granules are spread all over the cytoplasm and are further segregated into daughter cells (*) during late anaphase. b) Granules are labeled with Vasa-DsRed expression, nuclear envelope with LaminB2-GFP, and plasma membrane with farnesylated GFP. *In vivo* movies were taken by epifluorescence microscopy where time is specified for each frame in the upper right corner. After cytokinesis, the nuclear envelope reassembles (arrowheads), and while some granules are

already located in the area where the nucleus is forming (arrow), a group of granules spread in the cytoplasm readopt perinuclear localization (*) within 6.8 minutes. Time is measured from late anaphase, not shown in the figure. c) Nuclear envelope reassembly was also visualized by confocal microscopy by expression of NUP155-gfp. Granules move directly (arrows) to the area where the nuclear envelope is reassembling (arrowhead) during cytokinesis within 3 minutes.

2.2 Perinuclear granules colocalize with nuclear pores

After following the nuclear envelope reassembly by reconstitution of the nucleoporin network, a more detailed analysis of the subcellular localization of nuclear pores with respect to germinal granules was performed.

Normally, mRNA is exported from the nucleus through nuclear pores. Once in the cytoplasm, the mRNA can be trapped or targeted to specialized transporting organelles, or it can bind to cytoskeletal elements that assist its transport to its ultimate destination [91]. It has been proposed that perinuclear granules are specific structures of germ cells, where RNA is either stored or translated. We hypothesized that RNA binding proteins present in germinal granules may trap mRNAs that are exported from the nucleus. Therefore, RNA helicases like Vasa could allow RNA translation. If this holds true, it is possible to expect that nuclear pore proteins responsible for translocation of mRNAs to the cytoplasm, colocalize with perinuclear granules in the nuclear envelope. In order to test this hypothesis, we analyzed the subcellular localization of endogenous Vasa and endogenous Nucleoporins by confocal microscopy of whole mount immunostainings of 16hpf zebrafish embryos (Fig. 7). During interphase, the components of nuclear pore complexes (NPC) Nucleoporins (NUPs) p62, p152, and p60 are localized to the periphery of perinuclear granules of different sizes (Fig. 7a). This observation reveals specific colocalization between nuclear pores and germinal granules in the nuclear envelope of zebrafish germ cells. Interestingly, NUPs expression is also visualized in a cup-shape covering distal areas of perinuclear granules (Fig. 7b), as well as in cytoplasmic granules that are not in contact with the nuclear

envelope (Fig. 7c). The latter observations indicate that interaction between NUPs and components of germinal granules do not necessarily depend on the nuclear envelope structure.

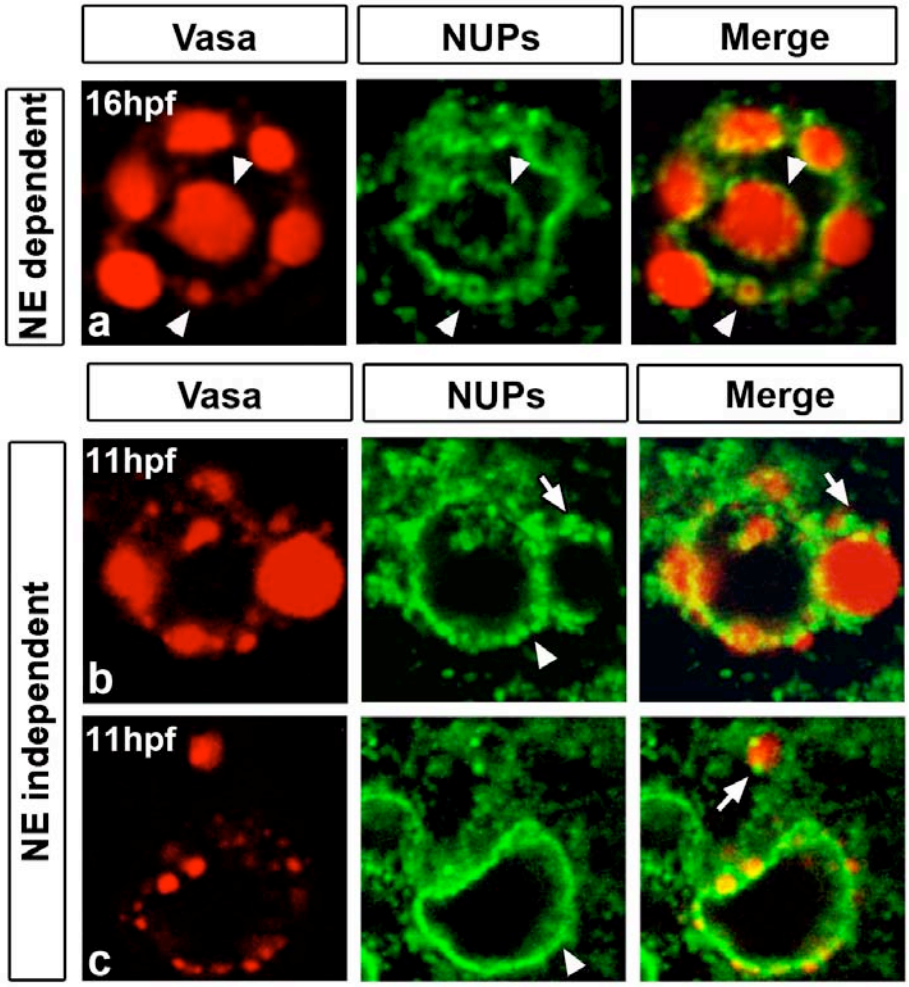

Figure 7. Germ cell granules colocalize with nuclear pore proteins in a nuclear envelope-dependent and a nuclear envelope-independent manner
Immunostaining of Vasa and nucleoporins p62, p152 and p60 of germ cells nuclei.
a) Granules located in the periphery of the nuclear envelope during interphase show specific colocalization with proteins that are part of the nuclear pore complex in 16hpf embryos. Arrowheads depict colocalization of both structures.
b) During interphase, nucleoporins not only are present in the nuclear envelope (arrowhead), but also forming a cup-shape like structure that surrounds granules, reaching distal areas that are not in contact with the nuclear envelope (NE).
c) Nucleoporins also colocalize with cytoplasmic granules (arrow) in a nuclear envelope-independent manner.

To test whether this organized colocalization persists throughout cell division, we followed these two structures after nuclear envelope disassembly by immunostaining of Vasa protein and Nucleoporins p62, p152, and p60. During early mitosis, the nuclear ring of NUPs diffuses, and perinuclear granules begin to detach from the disassembling envelope, yet still showing direct colocalization (Fig. 8a). At later stages of mitosis when the nuclear envelope is completely disassembled (Fig. 8b), NUPs and granules are distributed throughout the cytoplasm, excluded from the center of the cell. Although both structures do colocalize, it is not possible to ensure that such overlap of expression is specific. The latter is due to the broad area covered by nucleoporins in the cytoplasm.

Taken together, these observations indicate that nucleoporins are not only in close proximity to germinal granules through their association with the nuclear envelope, but they also colocalize in a nuclear envelop-independent manner. Specific colocalization can be seen also during early stages of mitosis while the nuclear envelope is disassembling. In later stages of cell division, NPC proteins colocalize with Vasa containing granules, although we cannot be certain that this is a specific colocalization.

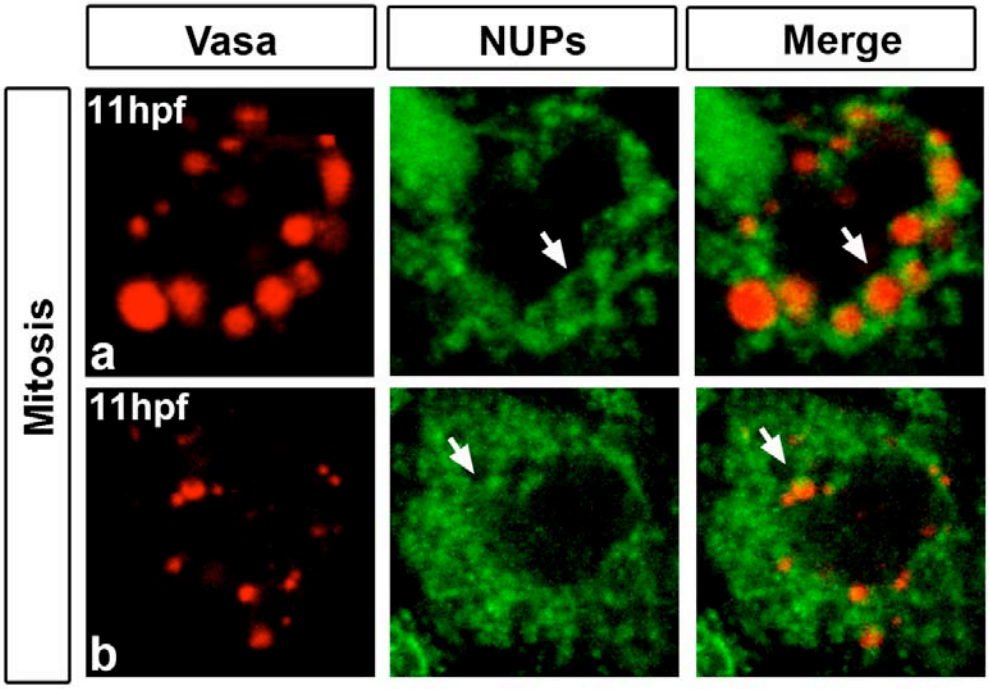

Figure 8. Colocalization of germinal granules and nuclear pore proteins during mitosis
Immunostaining of Vasa and Nucleoporins p62, p152 and p60 of germ cells nuclei.
a) During early mitosis, the nuclear envelope disassembles, and the characteristic NUP ring seen in Fig. 7b,c gets diffuse. Granules lose their perinuclear localization although they are still in colocalization with NUPs. b) Later during mitosis when the nuclear envelope is completely disassembled, perinuclear granules and NUPs extend throughout the cytoplasm primarily avoiding the center of the cell where chromosomes locate.

2.3 Cytoskeleton and perinuclear granules during cell cycle progression

During cell division, organelles and molecules are segregated into the forming daughter cells. When the component to be segregated is essential and is not abundant, the cell must ensure that after mitosis partition between daughters is either even or roughly equal. In this way, the cell avoids a situation in which one daughter cell may receive no copies of the essential component [87].
We previously showed that germ cell granules readopt perinuclear localization after termination of cell division. Considering this observation and the critical role the granules play in germ cell development [16], we asked whether granule distribution into the forming daughter cells is regulated by a cellular mechanism.
It was previously described that compartmentalization of germ plasm in early stages of zebrafish embryogenesis depends on microtubules [29]. In order to determine whether the distribution of perinuclear granules is also associated with these cytoskeleton components later in development, we analyzed microtubule distribution with respect to germinal granules throughout the cell cycle.

2.3.1 Microtubules and germ cell granules during interphase

Confocal immunostaining pictures of a germ cell during interphase revealed strong colocalization of Vasa-expressing granules with microtubular structures localized in the nucleus (Fig. 9a, see detail) of 6hpf embryos germ cells. As shown in detail in figure 9b, α-Tubulin staining could also be observed within the

perinuclear granule itself in germ cells of 16hpf embryos. The same is shown for 6hpf (Fig. 9a) and 11hpf (Fig. 9d) embryos.

To confirm the specific colocalization of Vasa-positive germinal granules and α-Tubulin, we labeled microtubules and Vasa by injection of *clip170-gfp-nos1*-3'UTR and *vasa-DsRed-nos1*-3'UTR RNA respectively. Microtubule dynamics and granule behavior was followed by *in vivo* confocal time-lapse microscopy.

As shown in figure 9c, germ cells of 11hpf embryos reveal a perinuclear cage of microtubules that originates from the microtubule-organizing center (MTOC) on one side of the nucleus. The cage appears to surround the complete nuclear area, where microtubules appear to traverse perinuclear granules in a random manner (Fig. 9c, see detail, movie 4). In addition, some cage microtubules project towards the cytoplasm, directly colocalizing with granules that are positioned in the vicinity of the nucleus in the cytoplasm (Fig. 9d, see detail, movie 5).

Given the results above, we asked whether MT colocalization with Vasa positive granules represents functional interaction between the structures. To address this question, we performed time-lapse microscopy analysis and followed dynamic behavior of cytosolic granules colocalizing with microtubules projecting from the MTOC in protruding germ cells. We found that while cytoplasmic granules that do not clearly colocalize with microtubular structures (Fig. 9e, arrow head) flow with the cytosolic stream into a forming protrusion (Fig. 9e, star), granules that associate with dense microtubule stripes are stabilized in their position near the nucleus. (Fig. 9e arrow, movie 6). This observation further supports the idea that cytoplasmic granules might interact with microtubules during interphase.

We conclude that perinuclear granules colocalize with microtubular structures at the nuclear envelope and in the nuclear periphery, strongly suggesting a possible function of this cytoskeleton component in either perinuclear granule function and/or structural maintenance.

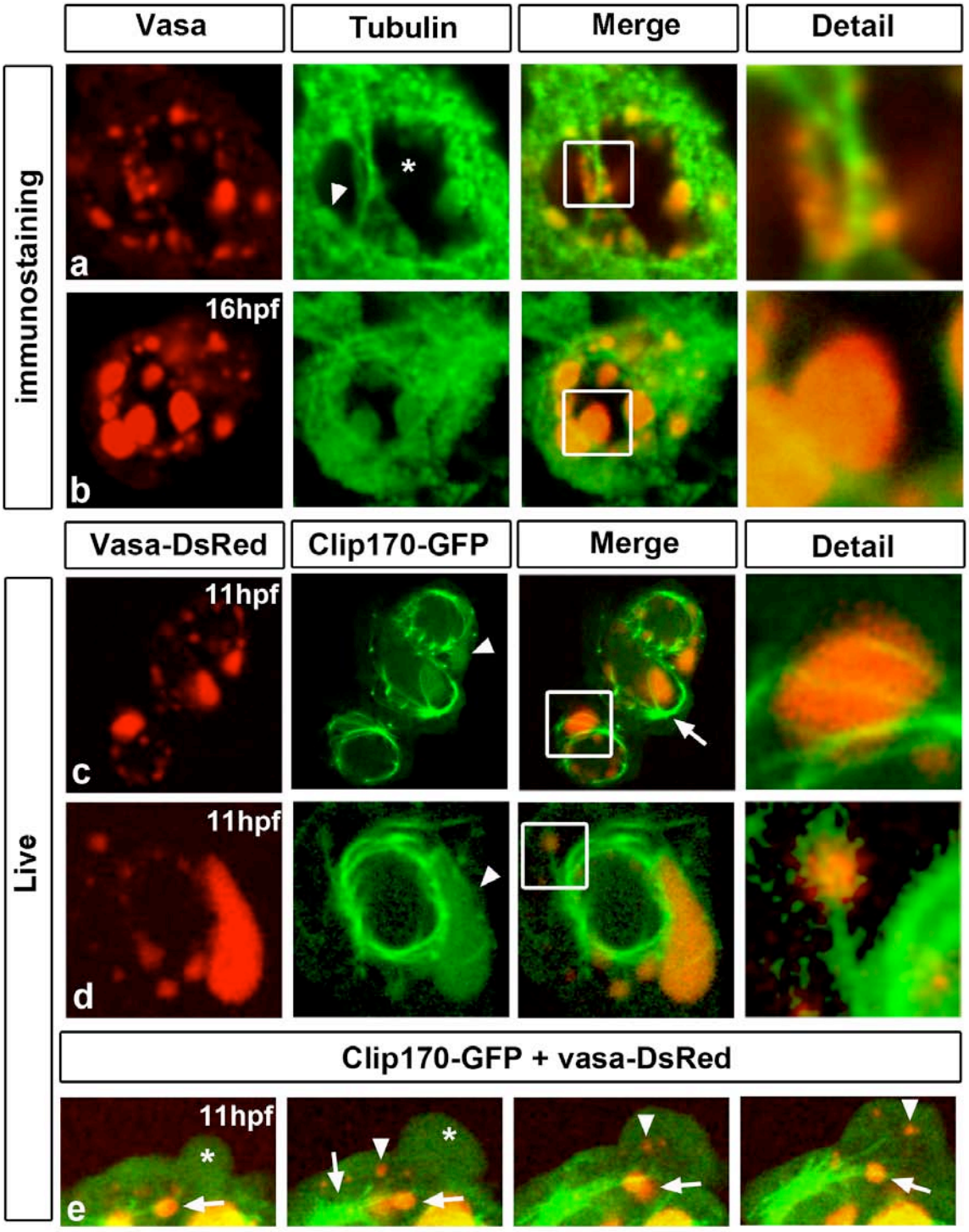

Figure 9. Microtubules colocalize and interact with germinal granules
a) Immunostaining of Vasa protein and α-Tubulin in germ cells of 6hpf embryos. Perinuclear granules attached to a microtubular structure in the nucleus are shown in detail. The asterisk and arrowhead depicts the nucleus and granules expressing Tubulin, respectively. b) At 16hpf, germ cell perinuclear granules also show expression of α-Tubulin (detail). c) Microtubules are labeled with Clip170-

GFP, and granules with Vasa-DsRed. *In vivo* time-lapse movies of 11hpf embryos reveal a microtubular cage surrounding three different germ cell nuclei, where microtubules span the granules (detail). d) Labeling as in c. Cytoplasmic granules colocalize with microtubular fibres projecting from the nuclear cage (detail). e) Close-up view of a protruding germ cell reveals flow of cytoplasmic granules (arrowhead) into the protrusion (asterisk) while others remain stable in colocalization with microtubules projected from the MTOC (arrow).

2.3.2 Dependency of granule structure on microtubule function

The presence of a perinuclear cage of microtubules that spans the granules raised the question whether this network functions as a structural support, keeping granules attached to the nuclear membrane. To address this question we exposed 7hpf embryos expressing Clip170-gfp and Vasa-DsRed to high concentrations of the microtubule-depolymerizing drug nocodazole (10μg/ml). Confocal pictures where taken after 30 minutes of exposure to the drug.

After disruption of the microtubular cage, the perinuclear localization and morphology of germinal granules remained unchanged (Fig. 10). These results indicate that the microtubular cage neither function as a structural support for the spherical shape of granules, nor to maintain their perinuclear localization.

It is possible that exposure to high concentrations of the drug for short time was not enough to disrupt completely all microtubular structures. In addition, such high concentrations seemed to affect proper development of the embryos. Therefore, we inhibited microtubules under lower concentrations of nocodazole for a longer period, and followed germ cells for more than one hour. 11hpf embryos expressing H1M-GFP labeled chromatin and Vasa-DsRed labeled granules where exposed to 1μg/ml of nocodazole where they grew for 4 hours. Germ cells where photographed by epifluorescence microscopy. As shown in figure 11b, Vasa positive granules appear to aggregate into one big structure, while control cells (Fig. 11a) exposed to DMSO exhibit normal perinuclear distribution of small granules.

In order to understand what lead to the phenotype obtained in the previous experiments, we exposed 11hpf embryos to the same conditions, but this time we followed germ cells by time-lapse microscopy. As shown in figure 11c, germ cells show normal distribution of granules around the nucleus when the drug was added to the medium (time 0). At 23.5 minutes after drug exposure, chromatin condenses as judged by an area reduction of the DNA marker H1M-GFP. At the same time, germinal granules conglomerate into bigger structures, without losing their perinuclear localization. After 57 minutes of exposure to the drug, perinuclear granules appeared to be larger in comparison to the ones observed at 0 minutes of exposure (Fig. 11c, movie 7). In order to determine the effect of microtubule disruption on the nuclear envelope, we repeated the same experiment labeling the nuclear envelope with LaminB2-GFP. As shown in figure 11d, after 55 minutes of exposure to the drug, the lamin matrix disassembled, spreading all over the cytoplasm. Simultaneously, once the nuclear envelope is no longer defined, granules fuse forming bigger structures.

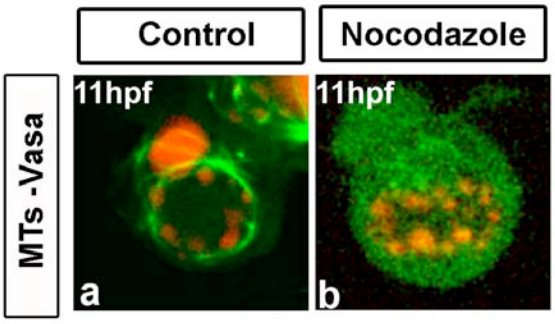

Figure 10. Transient disruption of microtubule function does not alter perinuclear localization of granules
a) A cage of microtubules surrounds the germ cell nucleus, visualized by clip170 and perinuclear granules by Vasa protein. Control embryos were exposed to DMSO for 30 min. b) 11hpf embryos were treated with 10μm/ml nocodazole dissolved in DMSO for 30min. Clip170 labeled structures are no longer visible and granules remain perinuclear. Cell in a) is not the same as in b).

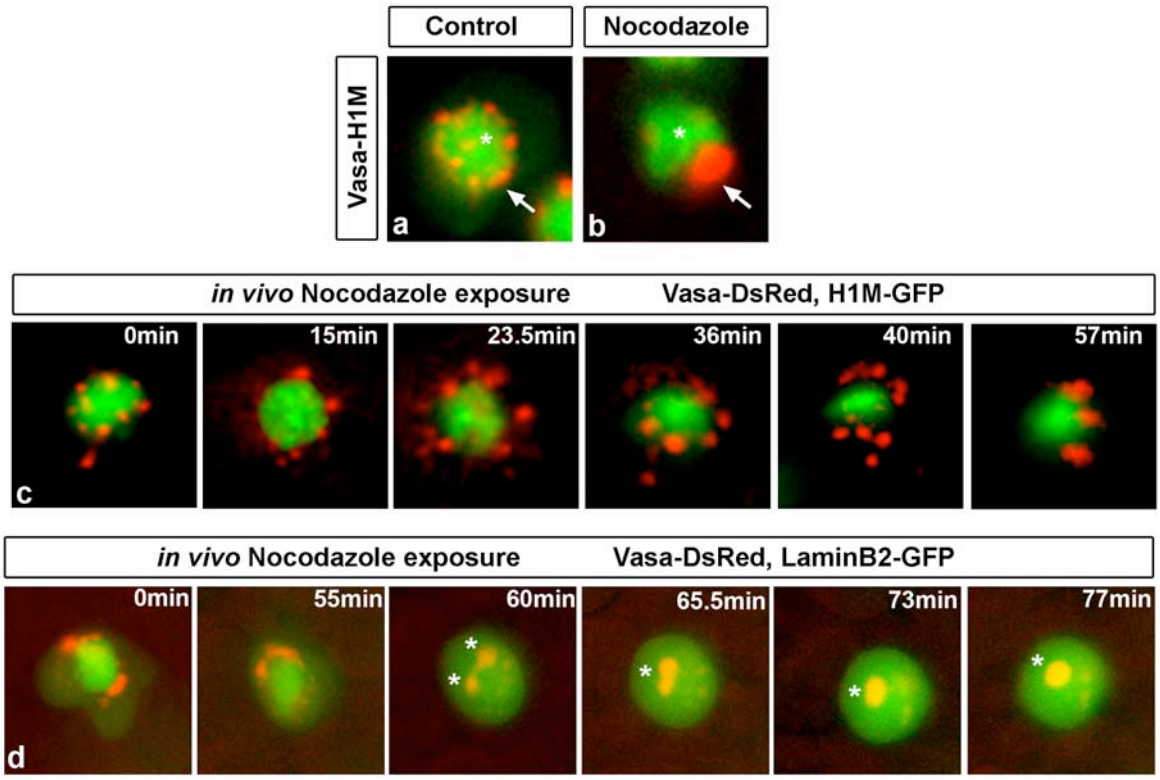

Figure 11. Granules structure is affected after persistent microtubule disruption

a,b,c) Exposure of 11hpf embryos to nocodazole was followed by *in vivo* epifluorescence microscopy. Germ cells are expressing H1M-GFP and Vasa-DsRed to label chromatin and granules respectively.

a) Confocal section of representative germ cells of control embryos exposed to DMSO for 6hpf. Vasa protein shows normal perinuclear localization with Vasa protein segregated into small structures. b) Confocal section of embryos exposed to 1μm/ml nocodazole for 4 hours. Nocodazole treated cells exhibit a conglomeration of Vasa positive granules around the nucleus. c). Due to bleaching of the fluorophores during the movie, colors in the three last pictures are enhanced in comparison to the time-lapse movie to properly visualize the structures (movie7). At time 0, germ cell granules show characteristic perinuclear localization, with normal average size. Associated with a reduction of the H1M labeled area, granules start to conglomerate, forming bigger structures when compared to cells at 0 min. d) 11hpf embryos exposed to same conditions mentioned above. Vasa-DsRed labels granules, LaminB2-GFP labels nucleus. The experiment shows how after laminB2 network disassembles, individual granules fuse forming bigger structures (*).

The results indicate that a short-lived disruption of the microtubular cage that surrounds the nucleus does not alter perinuclear localization of germinal granules. However, with continuous disruption of microtubular structures granules lose their individual structure and bind together into bigger spherical complexes. This suggests that microtubules and nuclear envelope components are crucial for proper structural maintenance of germinal granules.

2.3.3 Microtubules colocalize with germinal granules throughout mitosis

Due to the fact microtubules interact with germinal granules during interphase, we wanted to known if such functional dependency existed also during mitosis. During cell division complex mechanisms that depend on microtubules ensure proper distribution of elements into the forming daughter cells. This is the case for several cell components such as chromosomes and the Golgi apparatus [40, 92].

Regarding the colocalization and structural function MTs have in respect to granules during interphase, we hypostasize that granules and microtubules also colocalize during cell division. If this assumption holds true, this specific interaction could serve as a mechanism for segregation of perinuclear granules into daughter cells and therefore, ensure the maintenance of the germline during germ cell proliferation. To address this question, we analyzed localization of granules during different stages of mitosis in respect to microtubules. Immunocytochemistry and confocal imaging were preformed on 6hpf zebrafish germ cells stained for Vasa and α-Tubulin. In order to preserve cytoskeleton structures and avoid crystal formation that may destroy microtubules, embryos were dehydrated and fixed with methanol. The latter was done due to the fact that cytoskeleton preservation is highly sensitive to changes in chemical environment.

During prophase, while duplicated centrosomes migrate towards the poles of the cell (Fig. 12a arrows), tips of microtubules that originated from centrosomes show colocalization with perinuclear granules located close to the nuclear area (Fig. 12a, see picture of other focal plane). In addition, α-Tubulin can be detected

within the granule structure (Fig. 12a, detail). During prometaphase, when the mitotic spindle apparatus is forming, some germ cell granules can be found between centrosomes, in strict colocalization with spindle MTs (Fig. 12b), also expressing α-Tubulin within their structure. During metaphase, some perinuclear granules localize to the spindle apparatus (Fig. 12c), while others do not show association with microtubular structures. However, all granules express α-Tubulin (Fig. 12c detail). As the microtubule network might not be completely preserved during fixation, we cannot be certain that granules that do not show colocalization with microtubules are indeed independent from these structures. During anaphase, while the spindle apparatus is stretched between both daughter cells, granules become enriched in the poles, proximal to the area where the nucleus reassembles (Fig. 12d). Interestingly, they appear to be in close association with astral microtubules projected from the MTOC (Fig. 12d detail). During late telophase, granules are found in close proximity to the last extension of the spindle apparatus that still connects the two daughter cells (Fig. 12e).

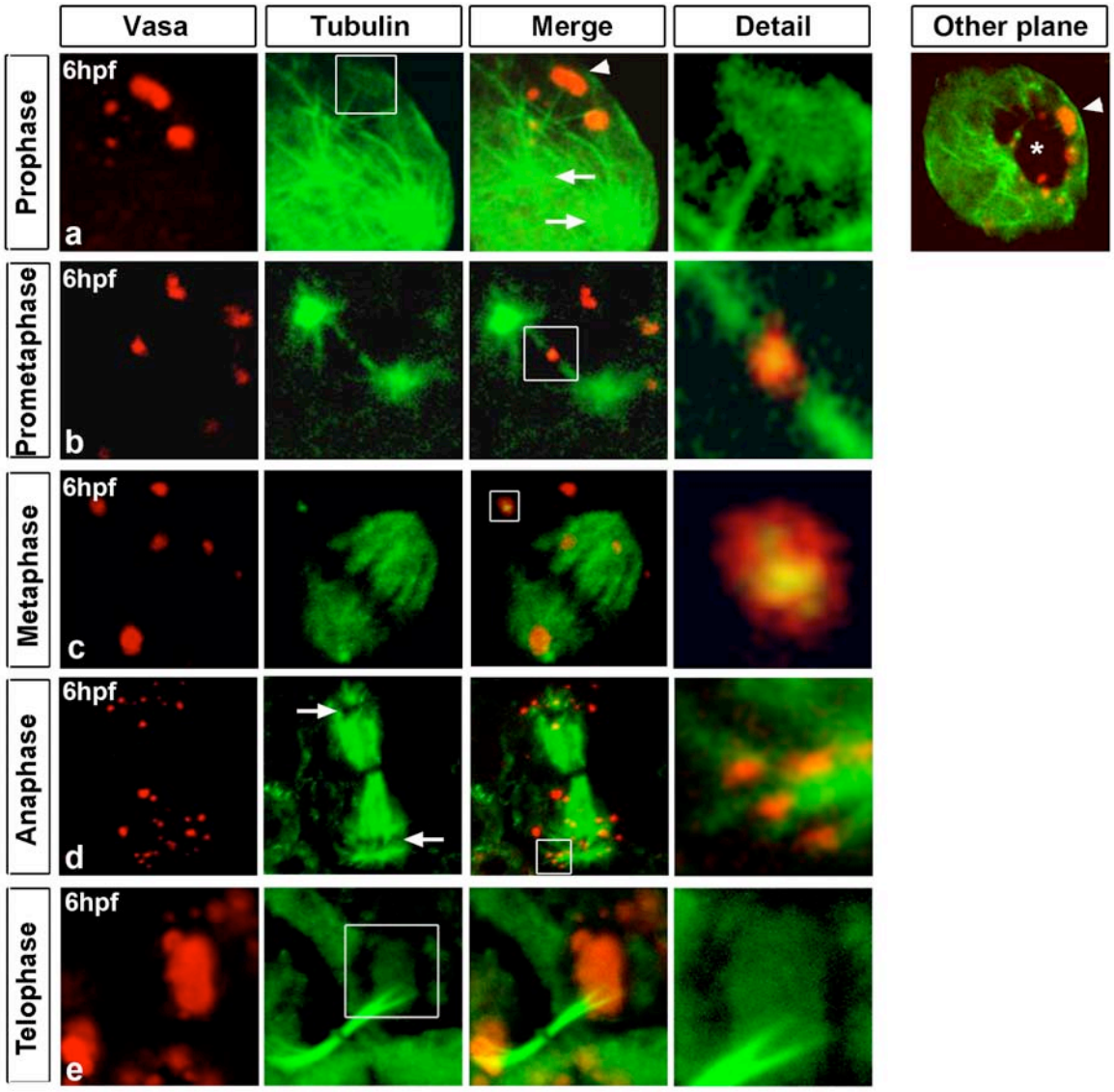

Figure 12. Microtubules associate to granules during different stages of germ cell mitosis

Immunostaining of germ cells undergoing cell division. Granules are labeled with anti-Vasa antibody, and microtubules with anti-α-Tubulin antibody.

a) During prophase, the spindle forms from the centrosomes (arrows). α-Tubulin-expressing granules (arrowhead in merge, detail) that are near the nucleus (* in other plane, arrowhead depicts same granule as in merge) appear in close association to microtubular fibers projecting from the centrosomes. b) In prometaphase, the two centrosomes are located in each pole of the cell, projecting spindle microtubules that colocalize with Vasa and α-Tubulin expressing granules (detail). c) During metaphase several granules localize to the spindle, while others do not appear in association with microtubular structures, but do express α-Tubulin within their structure. d) During anaphase, the spindle apparatus is distributed between both daughter cells and granules are enriched around the area where the nucleus starts to reassemble (arrows).

Specific colocalization of granules with astral microtubules is shown in detail. e) During telophase the last extension of the spindle that connects the daughter cells appear to be in association with germinal granules.

Given that Vasa and α-Tubulin immunostaining revealed colocalization of germinal granules with spindle microtubules, we investigated whether *in vivo* dynamics of perinuclear granule segregation would reveal more information into this same direction. For this purpose, we labeled microtubules, nucleus and germ cell granules by injection of *clip170-GFP-nos1* 3'UTR, *nupl1-GFP-nos1* 3'UTR and *vasa-DsRed-nos1* 3'UTR RNA, respectively. *In vivo* microtubule dynamics and perinuclear granule behavior was followed by confocal time-lapse microscopy in 10hpf zebrafish embryos.

During anaphase, perinuclear granules move directionally and continuously towards the forming nucleus within 1 minute, along a track that coincides with the spindle extension (Fig. 13a, movie 8). Elongation of their structure can be seen while they move from one cell to the other, re-adopting their spherical shape once they reach the area where the nucleus reassembles. Since germ cells nucleus in figure 13a was not labeled, we followed the same event in germ cells expressing Vasa-DsRed and NUPL1-GFP in order to visualize nuclear formation (Fig. 13c, movie 10). Consistent with our previous observations, granules may dynamically move within 1.3 minutes towards the area where the nuclear envelope is reassembling visualized by NUPL1 (total time of germ cell division is approximately 14 minutes). This time appeared to be shorter that the one described in section 2.1, where relocalization of all granules was described to last for 3-6.8 minutes. In addition to such mobile granules, it can also be observed that other granules remain stabilized close to the reassembling nucleus at the end of division (Fig. 13c, movie 10). Similar event is shown in figure 13b where larger granules can also move along the spindle extension in late telophase, while others appear to be stabilized by astral microtubules (Fig. 13b, insert, movie 9).

As a whole, these observations suggest a role of spindle and astral microtubules in germinal granule segregation and in positional stabilization of these structures during cell division. This conclusion could not be addressed by functional experiments such as microtubule depolymerization, since once the microtubular network is disrupted mitosis is arrested.

As previously mentioned, granules move towards the nuclear area after termination of cell division. To rule out the possibility that the contraction of the cytokinetic ring might be the force driving re-localization of the granules to the nucleus, we analyzed cells of embryos injected with dominant negative RhoAN[19]. The latter cells are unable to form a contractile actin ring during cytokinesis due to the lack of functional RhoA, a protein known to regulate acto-myosin contraction [93, 94]. As shown in figure 14, binucleated germ cells show normal localization of germinal granules to the periphery of the nuclear envelop at the end of mitosis. This is also demonstrated during interphase cells, which fail to segregate their cytoplasm after cell division.

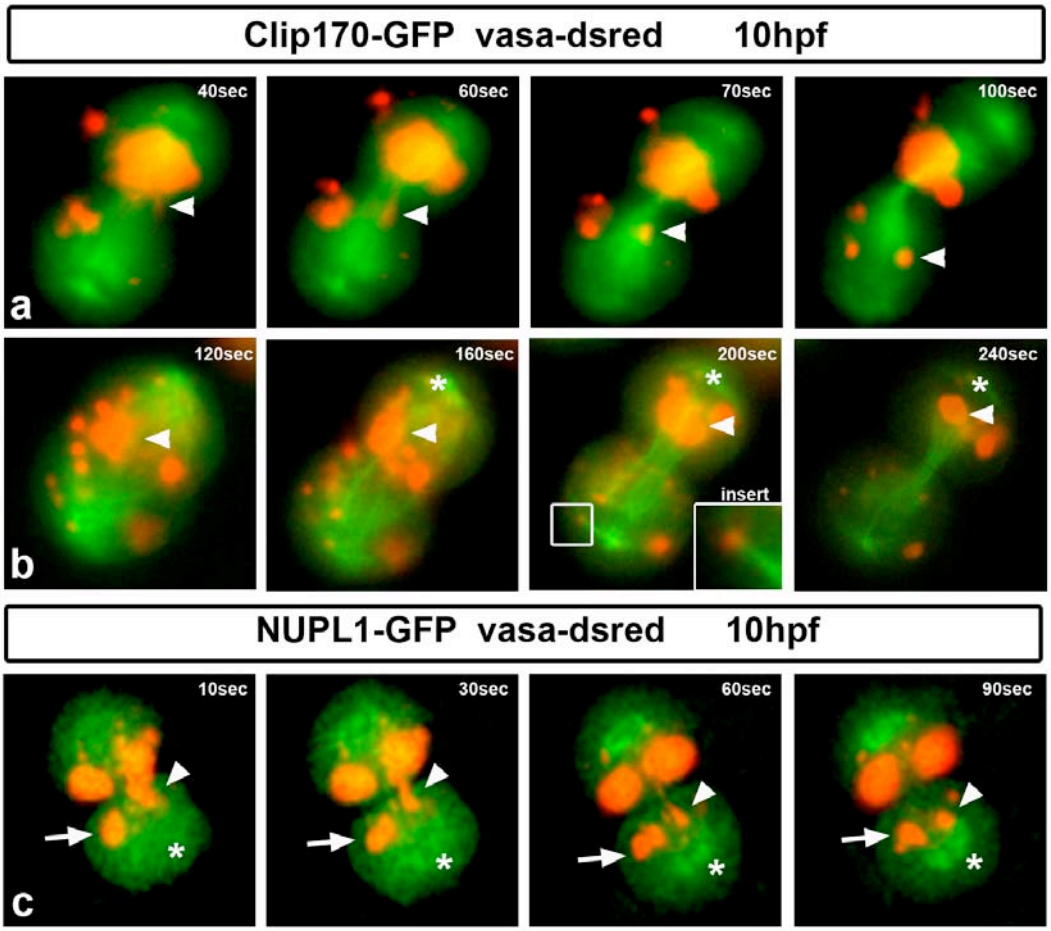

Figure 13. *In vivo* dynamics of germinal granules and microtubules during germ cell division

a) Vasa expressing perinuclear granules appear as elongated particles (arrowhead) moving from one daughter cell to the other on microtubule tracks. Once the granule reaches the area where the nucleus forms (shown in c), it re-adopts the spherical shape. b) Bigger germinal granules (arrowhead) move towards the forming nucleus (*) through a path of spindle microtubules. The colocalization of a granule with an astral microtubule is shown in detail (square, insert). c) In order to confirm that granules are mobilized from one daughter cell to the other directly to the area where the nucleus forms, nuclear envelope reassembly was visualized by NUPL1. Elongated granules (arrowhead) move from the cytokinetic region to the site of the forming nucleus (asterisk), re-adopting spherical shape upon arrival in a perinuclear position. Other granules remain stabilized in their original position in close proximity to the forming nucleus (arrow).

2.4 Distribution of the amount of germ plasm material during cell cycle progression

Subsequently and in order to support the hypothesis of a non-random mechanism in granule segregation during germ cell division, we calculated the number of granules populating each daughter PGC after completion of mitosis.
As shown in table 1, inheritance of granules by daughter cells after division shows a distribution of 50% with an average difference of 3%, from a total of 13 germ cells analyzed. More specifically, 5 cells inherited the same number of granules, while 8 showed a distribution of ± one granule per cell when the total number of granules is calculated (Table 1). This result suggests that segregation of germinal granules in zebrafish germ cells during mitosis is not a random process, supporting the idea that there is a controlled mechanism involved in the inheritance of these structures.

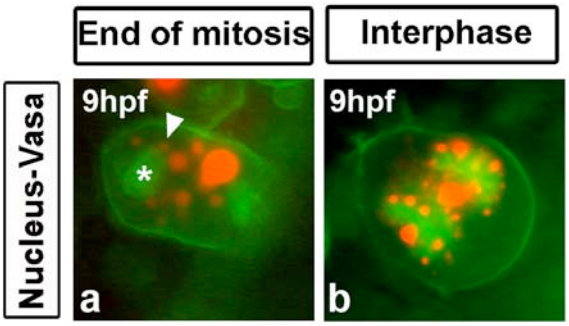

Figure 14. Inhibition of cytokinesis does not interfere with perinuclear relocalization of granules
Epifluorescence pictures of germ cells labeled with Farnesylated-GFP, H1M-GFP, Vasa-DsRed. a) Cells expressing RhoAN[19] cannot undergo cytokinesis. Hence, cell division is not completed and polynucleated cells are formed. Although there is no cytokinetic ring, granules are able to encounter the nuclear envelope (*) and readopt perinuclear localization (arrowhead) after cell division. b) Interphase cells show normal perinuclear distribution of germinal granules in both nuclei after abnormal termination of cell division.

In the previous analysis we describe the total number of granules segregated into each daughter cell after mitosis (from 6hpf to 10hpf). While performing this analysis, we noticed that although the number of granules segregated per cell is the same, the amount of material is not necessarily equal between daughter

cells. This is due to the high diversity in granule size. As shown in figure 13 and 15, it is frequently observed that after cell division, one daughter cell inherits more amount of material (larger granules) in comparison to the other cell (Fig. 15, movie11). The latter observation is particularly interesting due to the homogeneous granule sizes observed in 24hpf embryos, showing roughly the same quantity of material. This indicates that there must be a structural transformation from larger to smaller structures, while development proceeds during early and later embryonic stages.

N° granules Daughter 1	N° granules Daughter 2	%Difference
11	10	5
10	10	0
11	10	5
7	6	8
13	12	4
9	9	0
9	8	6
9	8	6
8	8	0
12	11	4
9	8	6
9	9	0
7	7	0
Average	**Average**	**Average**
9.5	8.9	3

Table 1. PGCs inherite identical number of granules after cell division

Percentage of granules inherited by each cell after mitosis. Vasa expressing granules of dividing germ cells were analyzed by *in vivo* time-lapse fluorescence microscopy. Total numbers of granules per daughter cell, and the difference in % are depicted in the table. A total of 13 cells showed equal distribution of granules per daughter cell with a average difference of 3%. (Daughter cell 1: 9.5 granules, daughter cell 2: 8.9 granules). Analyses where performed on 6-10hpf embryos

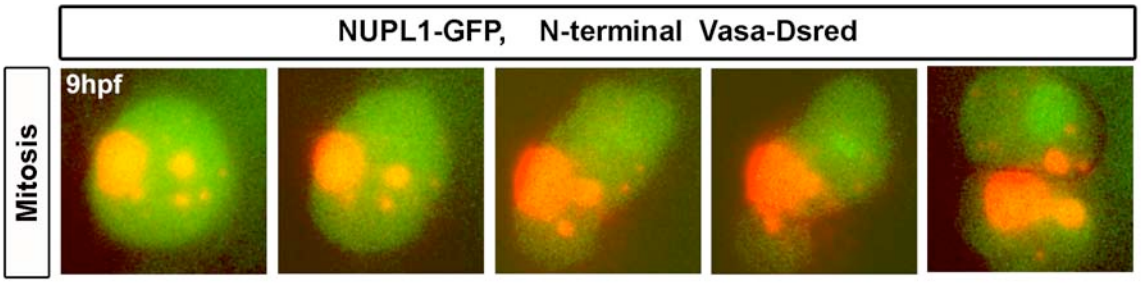

Figure 15. Asymmetric distribution of germ plasm material among daughter cells during mitosis (see next page)

Epifluorescence pictures of a germ cell expressing NUPL1-GFP and Vasa-DsRed. During cell division, germ cells may present an asymmetrical distribution of germ plasm material, where one daughter cell inherits more material than the other.

This finding raised two questions: 1. How does the asymmetrically inherited material become homogenously distributed at 24hpf, with all granules having approximately the same size? 2. How do cells that inherited less or more material reach similar levels at 24hpf?

In order to answer the first question, and to understand the structural process that leads to smaller granules with homogeneous sizes, we first characterized germ plasm material distribution from 4hpf to 24hpf of zebrafish germ cell development.

During early stages of development (before 6 hpf) specific labeling of the perinuclear granules is not possible primarily due to high signal background in somatic cells. To overcome this problem, we made use of a transgenic fish line that expresses the specific germinal granule protein Granulito fused to DsRed which allowed granule labeling as early as 4hpf sphere stage (unpublished data).

We documented germinal granules in PGCs of transgenic fish at 4hpf using confocal and epifluorescence microscopy. During early stages of germ cell development, the germ plasm appeared as several big spherical structures and smaller granules were rarely observed (Fig.16a).Interestingly, analysis of 9hpf embryos reveals a great diversity of granule size among different germ cells within the same embryo, where smaller structures appear to be more abundant as compared to early stages (Fig.16b). As previously mentioned, this heterogeneous distribution of the material becomes highly homogeneous at 24hpf in all germ cells (Fig.16c). These observations support the idea that a structural transformation of granules occurs during PGC development.

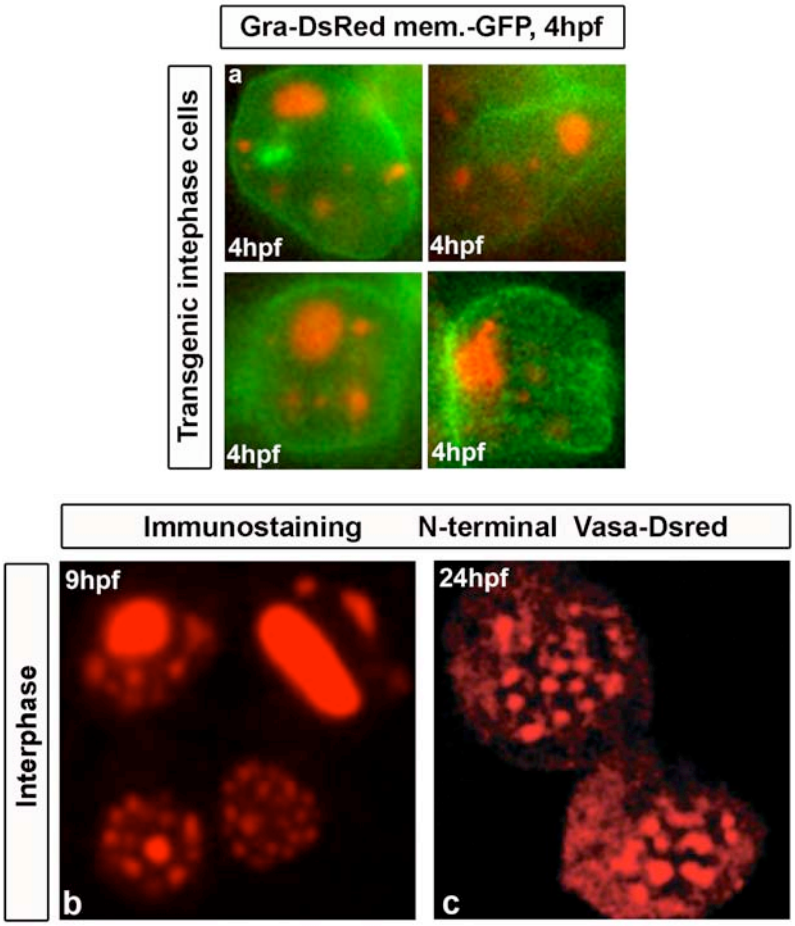

Figure 16. Granule size decreases during germ cell development from 4hpf to 24hpf

Germ cells expressing germ plasm markes during different stages of development.

a) *in vivo* pictures of four different cells of 4hpf transgenic embryos expressing granulito–DsRed that labels granules, and farnesylated-GFP labeling membrane. Big conglomerates of germinal granules appear to be more abundant than smaller structures. b) Immunostaining picture shows four different germ cell nuclei within the same embryo stained against Vasa protein. During 9hpf, germ cells show high diversity of germinal granules size among different interphase cells of the same embryo. c) Immunostaining picture of two different cells within the same embryo stained with anti-Vasa antibody. At 24hpf, germ cells show a homogeneous distribution of granule sized during interphase.

2.5 Recovery of Vasa protein after photobleaching in wild type germ cells

Subsequently, we aimed to answer the question of how do cells reach comparable levels of granule material at 24hpf, even if they inherited less when compared to the daughter cell during early stages of development?

A possible explanation for the fact that a similar quantity of material is found in PGCs at 24hpf is that cells synthesize germ cell granule material *de novo*.

To test our hypothesis, we performed *in vivo* fluorescence recovery after photobleaching (FRAP) of granules in 20hpf embryos labeled with Vasa-GFP protein. It was technically not possible to perform these experiments in early stages given that the signal intensity was not high enough for confocal microscopy. Four bleaching periods of 1 minute each were necessary to reduce Vasa-GFP intensity of one perinuclear granule to 42%. A representative experiment is shown in figure 17, where Vasa-GFP protein is able to recover up to 90% of its fluorescence intensity within 40 min. Fluorescence intensity of plasma membrane remained stable during the experiment, which served as an internal control (Fig. 17). These results indicate that granules are dynamic entities where turnover of granule material may occur, as demonstrated for the Vasa protein.

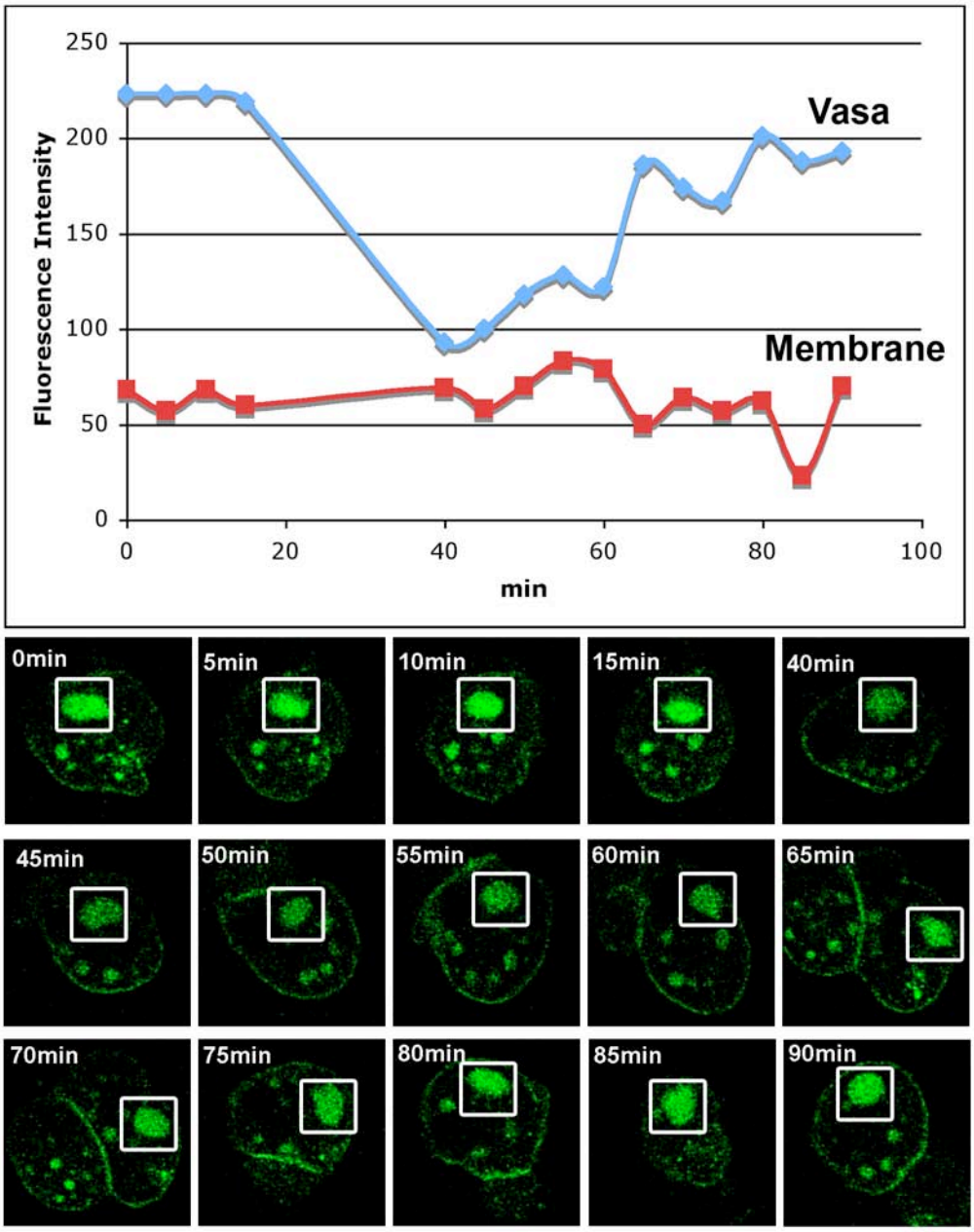

Figure 17. *In vivo* Vasa-GFP recovery after photobleaching in germ cell granules
A germ cell granule expressing Vasa-GFP (depicted with a square) was exposed to four photobleaching periods (1 min) and GFP intensity was reduced to 42%. Recovery was followed by confocal microscopy pictures every 5 minutes. Farnesylated-GFP labeling membrane within the same cell was used as control.

2.6 Role of the minus-end molecular motor dynein in granule structure

Once we demonstrated that granules have dynamic turnover of their components, we were interested in identifying possible molecules involved in transport of granule components. Given that microtubules and α-Tubulin colocalize with perinuclear granules during interphase (Fig. 9), we hypothesized that molecular motors may utilize microtubules in order to transport granule material, thereby regulating granule size and position within the cell.

To test this hypothesis, we tested the zebrafish *dynein light chain* (*DynL2*), a component of the multisubunit microtubule minus end-directed motor protein Cytoplamic Dynein, and the microtubule plus end-directed *kinesin11* (*Kif11*) for their subcellular localization. GFP fusion proteins of both genes were specifically expressed in germ cells through the fusion with *nos3'UTR*, and analyzed at 10hpf using fluorescence and confocal microscopy.

As shown in Figure 18a, Kif11-GFP localizes weakly to germinal granules and therefore it was not clear if such colocalization was specific. In contras DynL2-GFP, is found in the nucleus and in the cytoplasm, but more importantly, is strongly localized to germinal granules. Interestingly, Dynein distribution is dynamic, varying from ring-like structures around the germ cell granules (Fig. 18b) or small dots within the granules (Fig. 18d), to less defined accumulations in association with granules (Fig. 18e,f). In general, DynL2-GFP was preferentially found to be localized to the larger granules within a cell (Fig. 18b,c,d,f).

Colocalization of DynL2-GFP with germinal granules is not restricted to granules associated with the nuclear envelope, as DynL2-GFP is also found in cytoplasmatic granules (Fig. 18c).

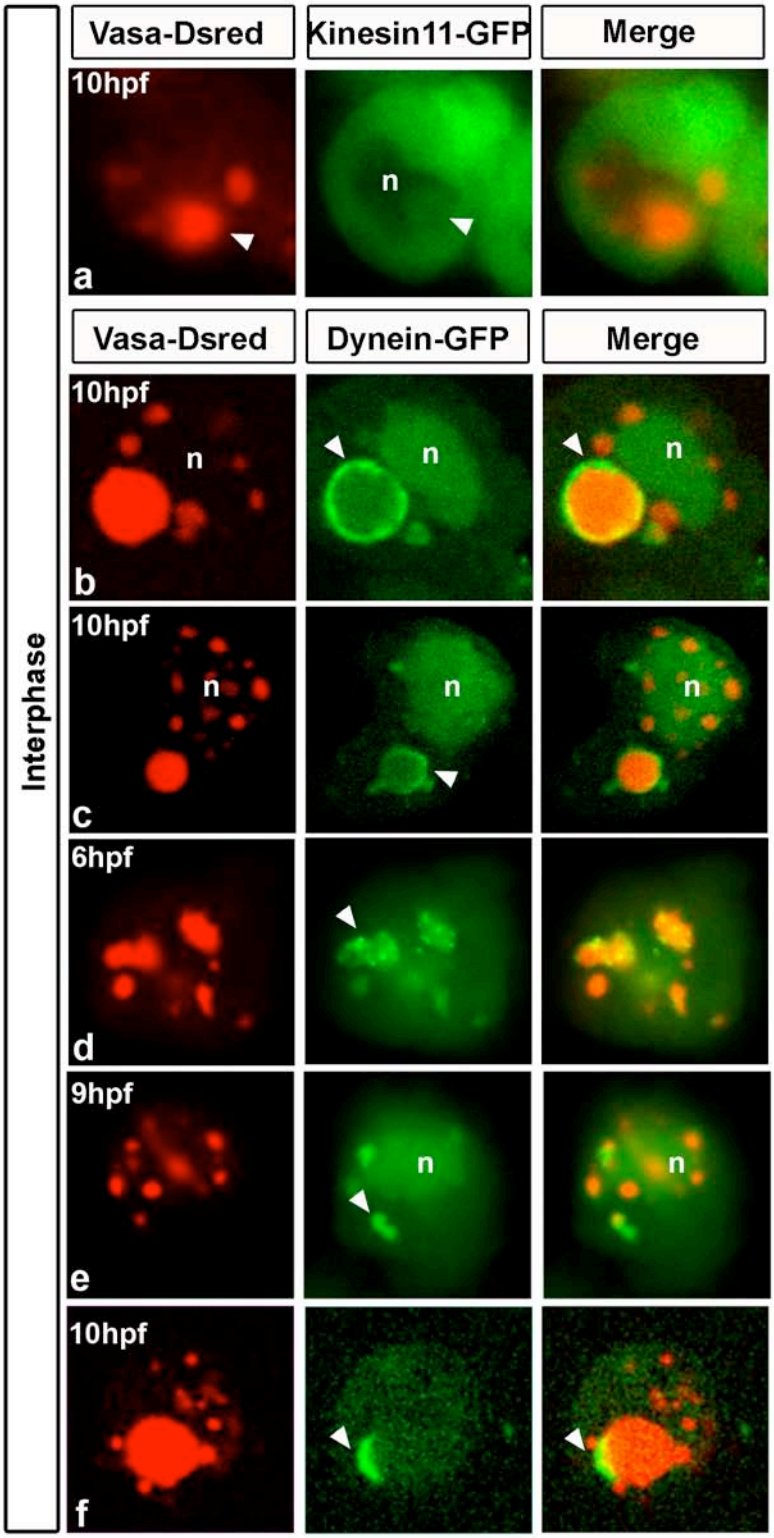

Figure 18. Kinesin 11 and Dynein light chain 2 like localize to germinal granules

Subcellular localization of micortubule-dependent motors. a) Kif11 is predominantly found in the cytoplasm and weakly localizes to germinal granules. b) DynL2-GFP is localized to nucleus, cytoplasm and to perinuclear and cytoplasmatic granules (c). Granule-specific DynL2-GFP localization patterns are diverse, ranging from ring-like structures around large granules (b,c arrowheads), dots within the granules (d), or granule-associated accumulations in the cytoplasm and nucleus (e). Nucleus is depicted by n. (f) DynL2-GFP accumulation can also be observed on the periphery of granules. Interphase cells where analyzed in 6, 9 and 10hpf embryos. Note that Vasa-DsRed and DynL2-GFP colocalization preferentially occurs in the largest granule of the cell, unless they all exhibit similar dimensions as seen in (e).

2.6.1 Dynein is necessary for proper germ plasm distribution within germ cells

Once we demonstrated that Dynein is localized to germinal granules, we analyze *in vivo* dynamics of the motor during interphase in order to get information of possible dynein function in granules. PGCs expressing DynL2-GFP and Vasa-DsRed at 9 hpf where monitored by time-lapse epifluorescence microscopy. As shown in figure 19, DynL2-GFP is initially strongly expressed in one big granule of the cell. The formation of an extension of DynL2-GFP precedes the division of a large granule; the granule division itself is additionally followed by a strong increase of DynL2-GFP concentration within the granule. (Fig. 19a-b, movie 12a green DynL2-GFP channel, movie 12b merge channels). This observation indicates that the motor Dynein may play an important role in the distribution of the granule material within the cell during interphase.

To obtain more information on this phenomenon, we followed germ cells labeled with fluorescent Dynein and Vasa this time by *in vivo* confocal microscopy. In figure 19c-d, we show that the specific ring that surrounds large perinuclear granules focuses within the granule forming a point of high dynein concentration. Once concentrated, DynL2-GFP moves towards the periphery of the granule until it detaches from it, carrying along Vasa containing material (Fig. 19c-d, movies 13a,c green channels, movies 13b,d merge channels). Although this event is different from the previously described in figure 19a,b it also supports the idea that Dynein is involved in germ plasm distribution within the cell by fragmentation of germinal granules. In agreement with this hypothesis is the finding that stronger DynL2-GFP expression is observed in big granules within cells (as in Fig. 18). This observation may reflect a higher requirement of Dynein function in granules that need to be fragmented.

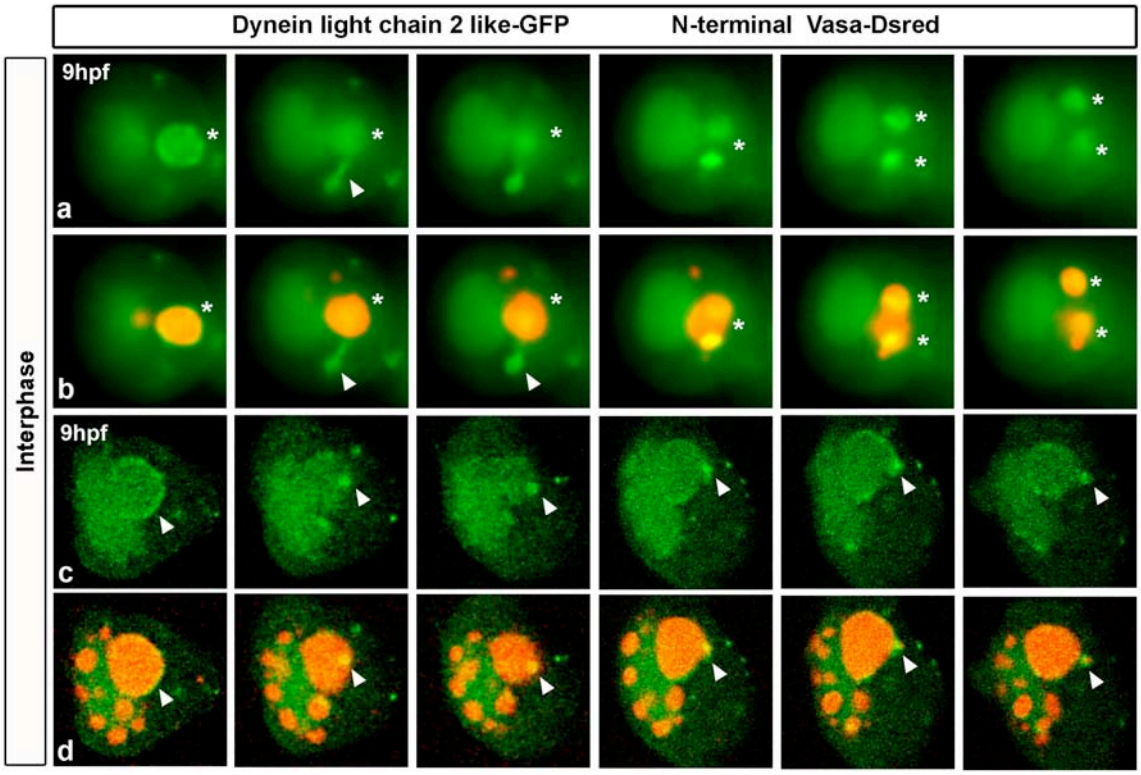

Figure 19. Dynein is involved in germinal granule fragmentation
Germ cells of 9hpf embryos expressing DynL2-GFP and Vasa-DsRed were analyzed *in vivo* by epifluorescence microscopy (a,b), or confocal microscopy (c,d). a) A DynL2 elongation reaches out of the granule (arrowhead), and precedes division of the granule. (*) See movie 12a. b) Merge of a) together with Vasa-DsRed red channel to visualize the granule (movie 12b).
c) Green channel showing DynL2-GFP localization in a germ cell. The ring-like localization of the motor concentrates into a speckle inside the granule (arrowhead) that moves towards the cytoplasm and exits the granule carrying along Vasa-containing material (movies 13a,b,c,d). (d) Merge of c) together with Vasa-DsRed red channel in order to visualize the granule (movies 13b,d).

Granule fragmentation is not limited to interphase cells, since large germinal granules may also be fragmented during cytokinesis, and separately distributed into daughter cells (Fig. 20a, movie14, also seen in fig.13c). Fragmentation of granules is also observed during late telophase, when granules reach the area where the nuclear envelope is reassembling (Fig. 20b, movie15). However, we cannot be certain that these processes during mitosis are also related to Dynein action since the motor was not labeled in the movies.

However, in addition to granule fragmentation, dynein appears to be taking an active part in granule distribution during cell division, as indicated by an

increase of DynL2-GFP intensity within granules. Such an increase in protein intensity coincides with the time granules translocate towards the forming nucleus of a daughter cell (Fig. 21, movie16a,b).

In section 2.1 we mentioned that wild type germ cells take approximately 14 minutes to undergo complete cell division. Note that primordial germ cells that overexpress DynL2-GFP take more time to complete division when compared to wild type (wt) PGCs (wt: 14 min, DynL2: 25.8 min). Dynein motors are involved in focusing minus ends of spindle microtubules at the poles and driving MT flux, and therefore, are implicated in normal spindle function [95]. It is possible that DynL2-GFP overexpression of causes a misbalance in spindle formation, with a consequent delay in mitosis. However, we report that PGCs are able to divide normally, reaching the normal number of cells at 24hpf.

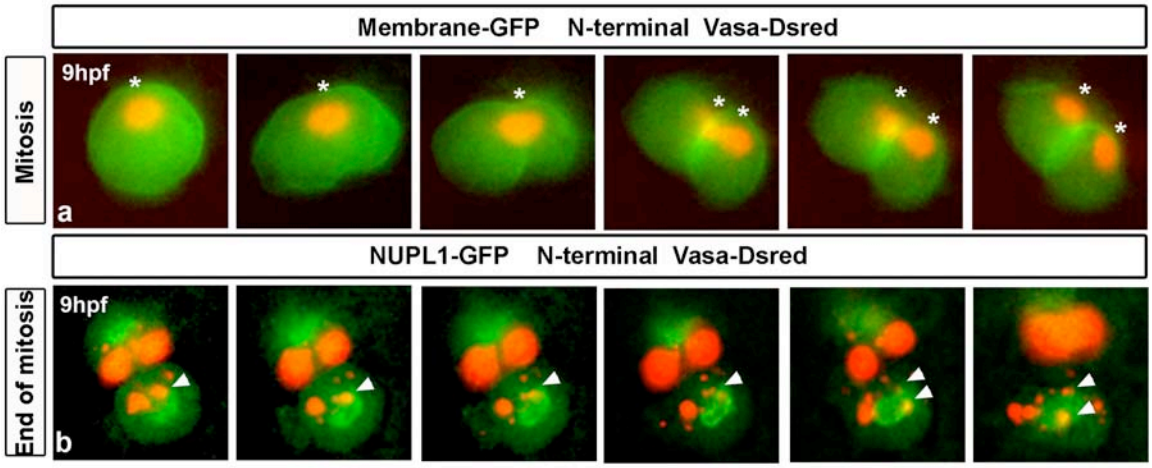

Figure 20. Fragmentation of germinal granules during and after cytokinesis

Germ cell granules can also be fragmented during or after cell division
a) Germ cells are labeled with membrane GFP and Vasa-DsRed. While germ cells undergo cell division, germinal granules may be fragmented and distributed among daughter cells (*). b) Germ cells are labeled with NUPL1-GFP and Vasa-DsRed. At the end of mitosis, germ cell granules may also be fragmented once they arrive to the newly formed nuclear envelope (arrowhead).

In conclusion, granules of larger dimensions are fragmented during development in a process that involves the microtubule minus end-directed

motor protein Dynein. Partition of large granules is also observed during cytokinesis of mitotic germ cells.

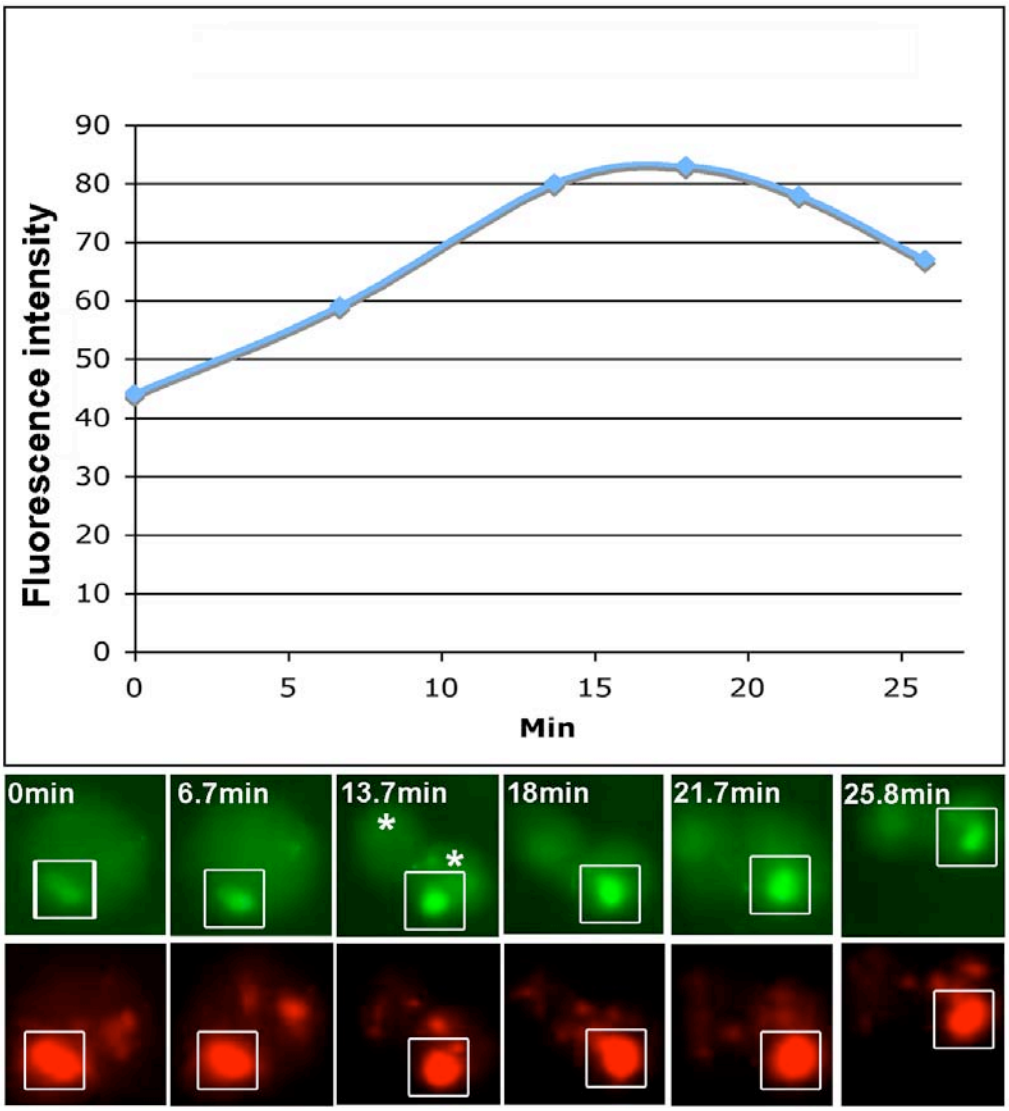

Figure 21. Granule translocation is associated with an increase of DynL2-GFP in germinal granules during cell division
Graph of fluorescence intensity and epifluorescence images of a germ cell expressing DynL2-GFP (White Square in green channel pictures) and Vasa-DsRed (white square in red channel pictures) undergoing cell division. Cytokinesis is observed during 13.7 and 18 minutes. During the translocation of the depicted granule to the nucleus of one daughter cell an increase in dynein-GFP intensity is observed. Dynein-GFP intensity decreases after division is completed at 25.8min. Daughter cells are depicted with an asterisk in 13.7min. Fluorescence intensity is given in arbitrary units.

2.6.2 Disruption of dynein function reveals improper granule distribution during interphase

Having established that dynein is specifically localized to the germinal granules and that it take part in structural changes of granules during development, we further investigated Dynein's functional role for proper granule distribution. We inhibited Dynein function by overexpression of the Dynactin subunit Dynamitin (p50) in germ cells [56]. Dynamitin overexpression is believed to disrupt the Dynactin complex, thereby inhibiting Dynein to bind its cargo [96].

As shown in figure 22, primordial germ cells of 24hpf embryos lacking functional Dynein show an abnormal distribution of total number of Vasa-positive granules. More specifically, germ cells of wild type (wt) embryos exhibit an average of 30 ±2.2 granules per cell, whereas germ cells that over express Dynamitin and therefore lack functional Dynein, show a statistically significant reduction of 50% in the total granule number (15 ±0.6 granules per cell, TTest $p < 2.55E-15$).

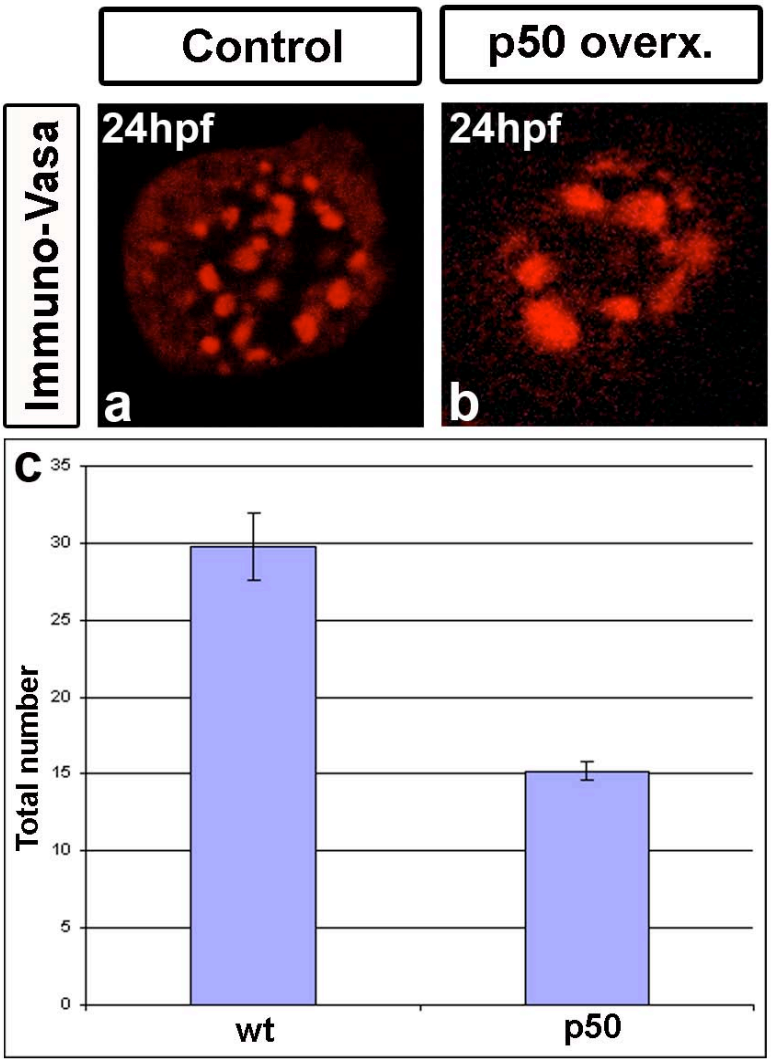

Figure 22. Dynein is involved in the regulation of the total number of germinal granules
a) Immunostaining of control germ cells show an overview of normal number of Vasa expressing granules per cell, where the average value is 30 ±2.2, in a total number of 33 cells analyzed. b) Dynein inhibition by p50 over expression reduces the number of granules per germ cell to 15 ±0.6, in a total number of 116 cells analyzed. c) Bar plot showing the corresponding total germinal granule number per experiment. Differences between control and both experiments are statistically significant (error bars: 2.2 control and 0.6 expreiment, TTest p< 2.55E-15).

Wild type values were obtained out of a total of 33 cells from 10 different embryos, whereas values for p50 overexpression were obtained out of a total of 116 cells from 20 different embryos. Total granule numbers were obtained by 3D reconstruction of germ cells stained with anti-Vasa antibody.

Moreover, we asked whether in addition of a reduction in granule number observed in p50-injected embryos, granule size is also affected. In order to address this question, we estimated the average area of germ cell granules of anti-Vasa antibody stained embryos. As the shape of germinal granules is not symmetrical, it is difficult to accurately measure their total volume. To overcome this problem, we calculated the area of the biggest granules from one plane of each cell. Hence, the values shown in figure 23 represent the circular area of granules obtained for controls and experiment by confocal sections.

We report that at 24hpf germinal granules of wild type germ cells have average values of 1.0 ± 0.1 μm^2 in size, whereas granules of cells lacking functional Dynein due to overexpression of Dynamitin, exhibit a total average of 2.1 ±0.2 μm^2. Difference between control and experiment are statistically significant (TTtest $p<5.8555E-9$)

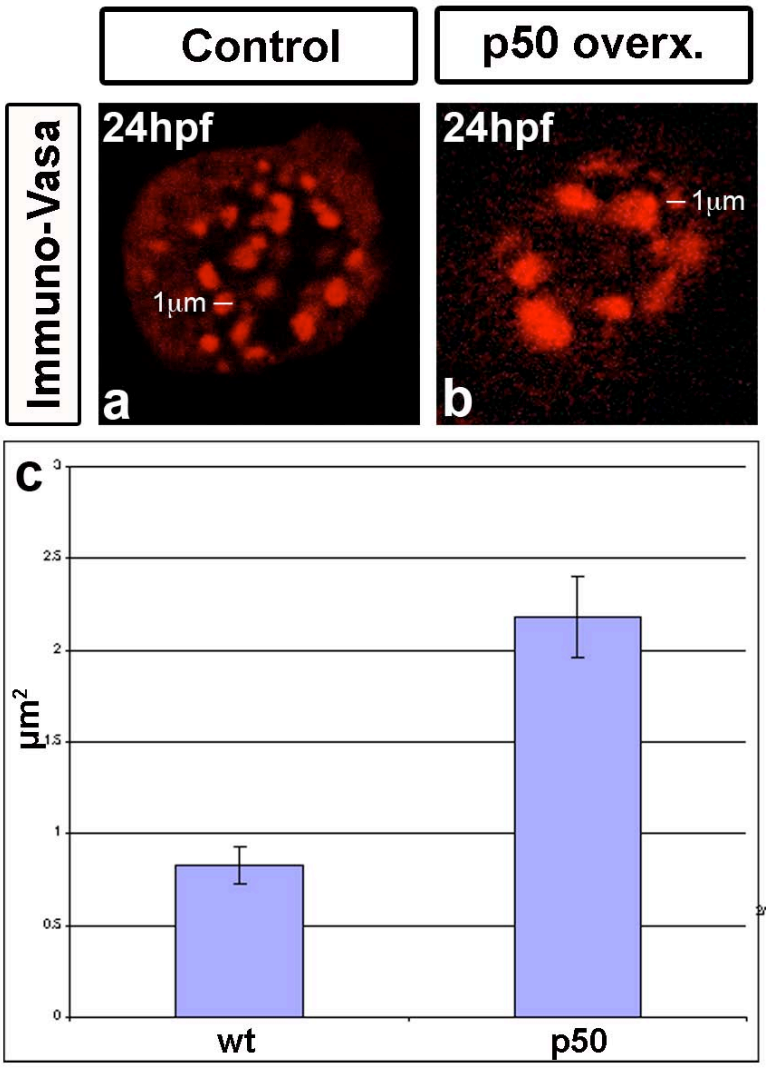

Figure 23. Granule size is dependent on Dynein function
a,c) Immunostaining of control germ cells show an overview of Vasa-expressing granules, exhibiting an average area of 0.8 ± 0.1 μm², in a total number of 191 granules analyzed. b,c) Dynein inhibition by p50 increases the size of germinal granules to 2.1 ± 0.2 μm², in a total number of 154 granules analyzed. Differences between control and p50 experiment are statistically significant (error bars: 0.1control and 0.2 expriment, TTtest p<5.8555E-9).

These results indicate that although cells lacking functional Dynein contain less number of granules per cell, germinal granules appear to be larger in size. Thus, inhibition of Dynein function confirms that the motor is involved in the proper granule size organization within the cell, during the first 24 hours of zebrafish embryonic development.

3.0 Discussion

Although germ plasm has been known for long to be essential and sufficient to promote germ cell fate, it still remains an enigmatic structure with many aspects of its function and structure yet to be studied and clarified. Specifically, it is not known how germ cells ensure proper distribution of germinal granules among daughter cells during cell division, and whether there is any change in germ plasm structure after the onset of zygotic transcription at 3.5hpf.

In this work, we address these questions and describe for the first time the distribution of zebrafish germ plasm during germ cells interphase and mitosis from 4hpf to 24hpf.

3.1 The role of microtubules in germ plasm segregation

In early stages of development while all cells proliferate, germ cells restrict their germ plasm only to one daughter cell, keeping their total number stable in the same four progenitors. This feature is achieved by the asymmetrical localization of the germ plasm components to only one pole of the dividing cell. Like this, only one of the two daughter cells will inherit the essential material that will specify it into a germ cell. At approximately 4 hours post fertilization (hpf) at sphere stage, PGC fate commitment is preceded by the translocation of RNA present in the germ plasm from its cortical to a more diffuse cytoplasmic location. A maternal program that is independent of zygotic transcription induces changes in germ plasm localization, with germ plasm proteins adopting a perinuclear localization [13]. Just after relocalization of germ plasm around the nucleus, germ cells start to proliferate as a result of equal distribution of germ plasm between daughter cells after cell division. Thus, accurate segregation of germ plasm is of great importance in order to avoid a possible loss of PGCs due to the lack of the determinant. Although the need for regulatory mechanisms that control the partition of germ plasm granules among daughter cells has been proposed [36], so far there has been no evidence for this.

At first, a series of studies have suggested that in zebrafish germ plasm components and microtubules function together in order to allow proper germ cell development and germ plasm segregation in early stages of embryogenesis. It has been known for *Xenopus* and *Drosophila that* the movement of germ plasm components during oogenesis depends on the formation of an organized microtubular network. After fertilization, germ plasm material localized at the vegetal pole of the oocyte forms aggregates in a microtubule dependent manner [97]. Similarly, aggregates containing *vasa m*RNA appear to be in direct contact with the outer tips of the microtubular bundles present in the cleavage furrows during the first two embryonic cleavages of zebrafish embryos [27]. The importance of microtubules for proper germ cell development was suggested when it was discovered that *vasa* mRNA fails to translocate to the distal cleavage planes in zebrafish embryos treated with the microtubule-depolymerizing drug nocodazole [29]. In line with this hypothesis, *vasa* mRNA mislocalization was observed in the maternal–affect *nebel* mutant, which exhibits defects of the microtubular organization at the cleavage furrows [27]. In addition to their importance for PGC development, microtubules were also implicated in the asymmetric segregation of germ plasm in later stages of development. During the 1000-cell stage, as presumptive zebrafish PGCs divide asymmetrically [8], germ plasm localizes to one of the two centrioles. This colocalization suggests a similar role of the spindle apparatus in asymmetric germ plasm partitioning in zebrafish, as it has been also proposed for *Xenopus* germ plasm segregation (Whitington and Dixon, 1975).

Since the previously mentioned studies have been done during the initial stages of development, we wanted to investigate whether the functional interaction of the microtubules and germ plasm occurs also during proliferative stages of PGCs. We extended our focus to the description of structural changes and behavior of germinal granules during all stages of germ cell proliferation and migration within the first day of development.

In interphase stages, germinal granules are localized around the nuclear envelope, where a microtubular cage surrounds the complete nuclear area (Fig.9). Interestingly, microtubules of this cage appear to traverse granules on the nuclear envelope and in the cytoplasm. Previous studies have described a

similar cage-like structure around the nucleus of neurons where cellular migration involves the coordinated movement of this cage and the centrosome [98]. As germ cells are also highly migratory cells, it would be interesting to investigate whether this structure is also involved in their migration process.

During nuclear envelope breakdown in prometaphase, germ cell granules lose their organized perinuclear configuration; the perinuclear cage of microtubules disassembles, and the spindle apparatus is formed. Retaining their spherical shape after detachment from the nuclear envelope, germinal granules appear to be scatter throughout the cytoplasm, yet remaining in close proximity to microtubular structures of the spindle. Throughout all stages of mitosis and cell divison, germinal granules colocalize with microtubules. These observations were corroborated by *in vivo* dynamics of granule segregation during germ cell division followed by time-lapse movies. Interestingly, granules can move from one daughter cell to another in what seems to be an active manner. Elongation of granule structure during mitosis is seen while they move from one daughter cell to the other, recovering their spherical shape once they reach the forming nucleus (Figure 13). The latter suggests that they might be subjected to a force that pulls them towards the area where the nucleus forms. Since not all granules move from one daughter cell to the other, several granules appear to be immobilized during cell division. These static granules appear to be in strict colocalization with microtubules of the spindle apparatus, once more suggesting that these structures may also play a role in granule positioning. During termination of cell division, granules regain perinuclear localization. Although the amount of material is not symmetrically distributed due to granule size variation, the number of granules that are distributed among daughter cells appears to be equal.

Two strategies could ensure such an accurate partitioning between daughter cells during cell divison [99]. A strategy known as ordered partition depends on association of the segregated material with the mitotic spindle. More specifically, all components to be segregated are attached to microtubules that control their equal inheritance among daughter cells. The stochastic strategy in turn, relies on random dispersion of an organelle present in multiple copies to ensure inheritance. These two strategies are not mutually

exclusive but may operate together particularly when the number of organelles is low [90]. Such a combination generates a much more accurate partitioning that would be expected from a stochastic mechanism, but not as accurate as an ordered one.

Germinal granules are accurately inherited by both daughter cells (equal or ± one granule per cell), suggesting an ordered partition mechanism (Table 1). Granules colocalize with microtubules during all stages of the cell cycle and seem to actively migrate along microtubule tracks during mitosis, suggesting a functional interaction (Fig.13). However, not all germinal granules appear in strict colocalization with microtubular structures during some stages of mitosis, indicating the presence of a stochastic component (Fig. 12). The missing colocalization of all granules with microtubules could in turn also be explained by the destruction of some microtubular structures upon fixation. In addition, all granules without exception showed colocalization with α-Tubulin within their structure, arguing for a general presence of microtubules in granules. At this point, we cannot assert that the missing colocalization of microtubules with some granules is an artifact of our experimental procedures. Since an additional effect of a stochastic distribution of granules cannot be excluded, a combination of an ordered mechanism with a minor stochastic distribution would be the best description of this segregation.

Hence, we propose that microtubules of the spindle apparatus are part of a mechanism that ensures inheritance of granules by daughter cells after cell division. In such a model, microtubules randomly encounter and bind some granules during centriole repositioning in prometaphase and chromosome capture in metaphase. Such an interaction is indeed present during prophase in germ cells when centrosomes are divided and move towards the poles (Fig.12). The model further suggests that granules remain attached to microtubules when the nuclear envelope disassembles and are pulled towards the forming poles by spindle microtubules. This allows a controlled segregation of the structures during the proceeding steps of mitosis, while those granules not captured by microtubules segregate in a stochastic manner. From an evolutionary aspect, it might not be surprising that this segregation mechanism is less precise than chromosome partitioning. Accordingly, a small imbalance in the distribution of germinal granules will

most probably not be lethal for the germ cell. Nevertheless, such combined mechanism might be sufficient to ensure enough germinal granules for each daughter cell, allowing downregulation of somatic genes and activation of germ cell specific ones.

Due to the essential function germ plasm plays in germ cell differentiation, it is reasonable to believe that germinal granule segregation during mitosis is as crucial for germ cell development and survival as the proper partitioning of other organelles. In other cell lineages, a segregation mechanism dependent on microtubules has been described for several organelles, where one relevant example is the distribution of the Golgi apparatus [92]. During mitosis, this organelle is transformed into highly dispersed tubulo-vesicular membranes proposed to facilitate stochastic inheritance of this otherwise low copy number organelle during cytokinesis [92, 100, 101]. However, this idea was reverted when it was described that Golgi inheritance is accomplished by an ordered partitioning mechanism that depends on spindle microtubules [92]. As shown in figure 24, partitioning stages of germinal granules appear to be highly similar to the segregation of the Golgi apparatus. During interphase the Golgi apparatus also appears in perinuclear localization (Fig. 24a) and spreads into the cytoplasm while mitosis proceeds (Fig. 24b-d), regaining perinuclear localization at the end of cell division (Fig. 24e). In addition, both structures exist in low copies in the cell [92]. As found for germinal granules, Golgi vesicles associate with astral microtubules, both proximal and distal to the spindle, strongly suggesting a role for microtubules in mitotic Golgi organization [92].

As mentioned above, Golgi vesicles regain perinuclear localization by a proposed microtubule-dependent mechanism. Such a mechanism could also explain perinuclear granule re-association with the nuclear envelope after germ cell division (Fig. 24a`-e`).

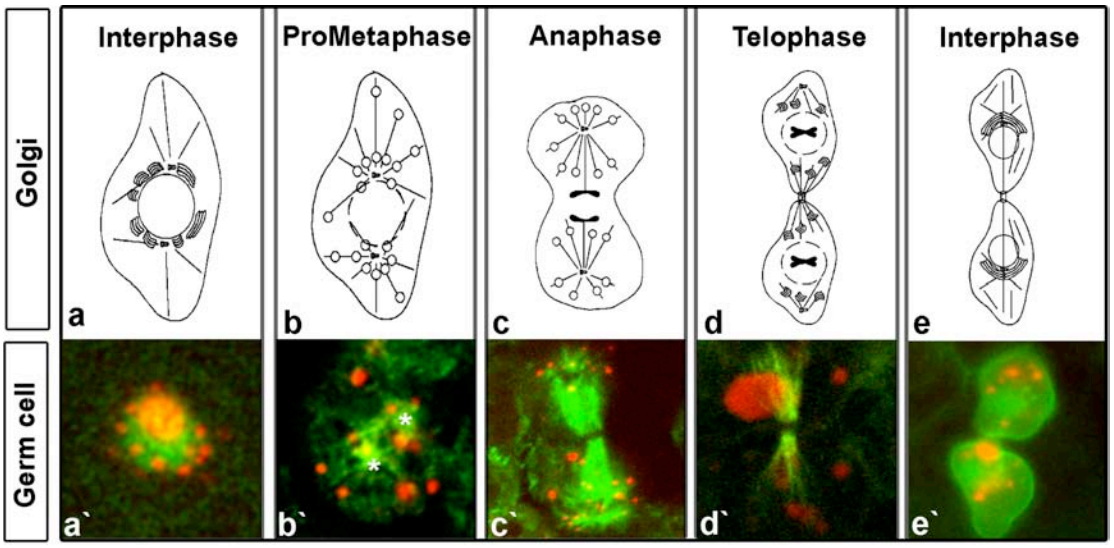

Figure 24. Golgi apparatus segregation compared to germinal granule distribution during mitosis
a) During interphase the Golgi apparatus is found at a perinuclear position, where it fragments into vesicles before the beginning of mitosis. b) Vesicles are distributed among daughter cells in colocalization with microtubules of the spindle during ProMetaphase. c) Vesicles are transported towards the forming nucleus, and accumulate around the centrosomes on each daughter cell during anaphase. d) In telophase, Golgi vesicles also localize to the final spindle extension that still connects the daughter cells during later stages of cytokinesis. e) After mitosis, Golgi vesicles readopt perinuclear localization and fuse into cisternae (Cartoon adapted from [92]). a`) Germinal granules are found in a perinuclear organization before division. b`) During ProMetaphase, granules are distributed among daughter cells in colocalizaton with spindle microtubules. c`) During anaphase, granules enrich around the splindle poles of each daughter cell in colocalization with spindle microtubules. d`) In telophase, germinal granules can also be seen in the final spindle extension after cytokinesis. e`) After mitosis, germinal granules readopt a perinuclear organization.

3.2 Structural maintenance and remodeling of germinal granules

Although the suggested model for germinal granule segregation microtubule-dependent precisely predicts our observations, a functional interaction between microtubules and granules has not yet been presented. Since microtubule dysfunction during mitosis leads to mitotic arrest, it is impossible to directly confirm the microtubule-dependency of granule segregation. However, experiments that investigated the granular structural maintenance

during interphase support the hypothesis of a functional dependency of granules on proper microtubule function.

3.2.1 Microtubules as a structural support for granules

During interphase, persistent inhibition of microtubule function using low concentrations of nocodazole leads to microtubule disruption, nuclear lamin network disassembly, and granule fusion (Fig. 11). However, transient disruption of microtubules with high concentrations of nocodazol does not show granule fusion (Fig. 10). Possibly, the short exposure to higher drug concentrations was not sufficient to properly depolymerize all microtubular structures. In support of this, the granule fusion was observed after approximately one hour. It should be noted that the granular fusion coincides with a collapse of nuclear structures, so an influence of the nuclear envelope on granule stability cannot be excluded. However, granule fusion is not observed after nuclear disassembly in mitosis, suggesting that microtubules prevent granule blend while the nuclear envelope is not present during cell division. We therefore conclude that the fusion of germinal granules after extended periods of microtubule depolymerization indicates that microtubules are indeed needed for structural integrity and distribution of granules.

3.2.2 Microtubule-dependent motor Dynein regulates granule size

As we imply microtubules to be necessary for proper segregation and structure, we investigated whether microtubule-dependent motor proteins mediate transport of germinal granules along microtubular tracks. The microtubule-dependent motor protein dynein is a minus-end directed motor, which appears to be specifically localized to germinal granules visualized by localization of DynL2-GFP (Fig. 18). In support of a motor protein-dependent granule transport, we observed increase intensity of DynL2-GFP signal in translocating granules during anaphase. Further experiments should be performed to verify a Dynein-germ plasm interaction and demonstrate specific germ plasm interaction partners with Dynein light chains.
Interestingly, the novel and unique *Xenopus* protein Germes*,* important for structure and behaviour of *Xenopus* germ cells, localizes specifically to germ

plasm and directly interacts with Dynein light chains [102]. The presence of germ plasm components that directly interact with Dynein motors in other species strongly supports the observations we describe in this work.

Besides granule mobility along microtubule tracks during mitosis, we also described a highly dynamic pattern of Dynein localization to germinal granules during interphase (Fig. 18). *In vivo* time-lapse microscopy confirmed that these different localizations represent active Dynein movement within these structures (Fig. 19). The experiments further suggest that Dynein is able to influence granule structure, participating in specific fragmentation of large granules during interphase. When strong DynL2-GFP accumulations are observed within granules, either new small vasa-positive granules form and separate from the large granules, or large granules are fragmented (Fig. 19). This observation leads us to believe that Dynein also plays a role during granular remodeling and transformation. We believe that throughout the first day of development, granule shapes and numbers change from few and very large structures within the first 4 hours to many small granules in one-day old embryos. Between 4hpf to 24hpf the total granule number per germ cell increases progressively, which is accompanied by a decrease of the individual granule size. In support of this hypothesis, disruption of Dynein function by Dynamitin over-expression results in larger granules. In addition, increased Dynein subcellular localization to large granules is consistent with the motor function within large granules that are transformed into smaller entities.

It has been demonstrated that proper number and structural organization of germinal granules is fundamental for normal germline development. One example of such statement is the function Tudor domains play in *Drosophila* polar granule formation. Tudor proteins have been described as docking platforms for proper granule structuring, flies with null mutations display a grandchildless phenotype: the progeny of mutant females are sterile [103]. Similarly, mutations in mouse Tudor related genes lead to male sterility due to postnatal spermatogenic defects [104]. However, if the abnormal granule structure caused by Dynein deficiency in zebrafish germ cells also impairs proper germ cell development and fertility remains to be elucidated.

3.2.3 Turnover of granule material

As we propose, microtubules and Dynein serve the purpose in a controlled mechanism to provide each daughter cell with the same number of granules. However, there are occasions when the germ cell material is unevenly distributed, and daughter cells inherit little amounts of it. This observation raises the question whether there is a minimum quantity of germ plasm that cells need to express in order to keep their germ cell properties, or to survive. We demonstrate by bleaching experiments that there is a constant flow of Vasa protein into germinal granules (Fig. 17). This can be explained either by *de novo* protein synthesis, or by relocation of material from other granules present in the same cell. This depicts granules as dynamic structures able to exchange or restore lost material. Given that germ plasm are continuously produced in germ cells, it is unlikely that germ cells would be lost along proliferative stages due to complete absence of germinal material. This is consistent with the fact that in the course of our experiments, we did not encounter living germ cells without germ plasm.

3.3 Nuclear pores and perinuclear granule colocalization

Nuclear pores are complex gateways on the nuclear envelope that control macromolecular transport between the cytoplasm and the nucleus. Interestingly, after structural analysis of germinal granules, we noticed that nuclear pore complexes (NPC) show strict co-localization with Vasa positive granules (Fig. 7). Such clustering of nuclear pores around germinal granules has been previously described also for *C.elegans,* however it occurs only in the adult hermaphrodite gonad [105].

The experiments presented in this work do not allow a conclusive statement about a functional significance between granules and NPCs, as a consequence of the colocalization of both structures. However, our observations suggest that neither germinal granules nor NPCs form at random sites of the nuclear envelope during the first day of embryogenesis. One possible functional event that would explain this colocalization is the entrapment of molecule complexes like messenger ribonucleoprotein particles (mRNPs), moving from the nucleus to the cytoplasm across the granules. It is

possible that once they are localized to granules, different germ plasm components become involved in remodeling their structure or regulating their translation. This hypothesis is supported by the fact that several germ plasm components like Vasa, Nanos and Dead end, are RNA binding proteins with RNA unwinding and regulatory functions [16, 35, 106]. Moreover, it has been described that newly exported mRNPs are not structured for proper translation, and therefore certain RNA helicases unwind short double-stranded regions of RNA, or dissociate bound proteins from RNA in order to allow translation [71]. Interestingly, it has been demonstrated in Yeast that the enzymatic machinery predicted to mediate mRNP remodelling during export is activated through critical interactions that occur at the NPC filaments located on the cytoplasmic side of the NPC. This is also the position where the germinal granules are located in zebrafish germ cells. Furthermore, it has been demonstrated that key factors involved in this process are members of the Vasa family. Taking together the previous statements, it is tempting to speculate that germinal granules may act as a receptacle of newly synthesized RNA molecules behaving as RNA processing complexes.

4.0 Materials and Methods

4.1 Bacteria

E. Coli Top 10F'	Invitrogen
E. Coli ElectroTen-Blue	Stratagene
E. Coli DH5a	Invitrogen

4.2 Chemicals

All chemicals, if not noted otherwise, were purchased from the companies Applichem, Merck, Roth and SIGMA

anti-DIG antibody	Roche 1093274
anti-fluorescein antibody	Roche 1426338
DIG RNA labeling Mix	Roche 1277073

4.3 Kits

mMessage mMachine Kit	Ambion
Topo-TA Cloning Kit	Invitrogen
UltraCleanTM 15 DNA Purification Kit	MO BIO
QIAquick Gel extraction Kit	Quiagen
Advantage HF 2 PCR Kit	Clontech
QIAquick PCR purification Kit	Qiagen
QIAfilter Plasmid Mini/Midi/Maxi Kit	Qiagen

4.4 Primary and Secondary Antibodies

Table 2

Lab No	Primary antibody	Specificity	Description	Company	Assay and used dilution
P1	Anti-GFP	GFP	Mouse monoclonal	Santa Cruz Biotechnolgy	Immunostaining 1:1000
P2	Anti-vasa K12/4	Zebrafish Vasa	Rabbit polyclonal	From Holger Knaut	Immunostaining 1:2000
P15	Anti-NUP	Conserved	Mouse	Covance	Immunostaining

		domain FXFG repeats in nucleoporins like the p62, p152, and p60	monoclonal	Research (Hiss Diagnostics)	1:1000
P26	Anti α-tubulin	α tubulin	Mouse monoclonal	Sigma	Immunostaining 1:1000

Lab No	Secondary antibody	Specificity	Description	Company	Assay and used dilution
S1	Alexa Fluor 488 (Green)	Goat-anti-mouse IgG	Alexa Fluor 488 conjugated Polyclonal	Molecular probes cat. A11001	Immunostaining 1:200
S6	Alexa Fluor 546 (red)	Goat-anti-rabbit IgG	Alexa 546 conjugated Polyclonal	Molecular probes Cat.A11071	Immunostaining 1:200

4.5 DNA Constructs used in this work

Table 3

DNA constructs made during this work		
Plasmid No.	**Name**	**Description**
A031	pSP64T-*laminB2-gfp-nos1*-3'UTR	LaminB2 fused to GFP and nos1 3'UTR for specific expression in PGCs. GenBank accession number NM_131002. Primers: 5'AAAGGATCCATGGCGACCGCAACCCCGAGCCG3' 5'AAAGGATCCCACCATCACTGCACATTCTCTGG3'

		Linearization and RNA synthesis: Apa1 and Sp6 RNA concentration for injection: 100ng/μl
A135	pSP64T-*vasaNterminal-dsRedEx-nos1*-3'UTR	N terminal fraction of Vasa protein sufficient to localize DsRed fluorophore to granules. Primers: 5'TAGGATCCAAATGGCCTCCTCCGAGGACGT3' 5'ATAGATCTAGACTACAGGAACAGGTGGTG3' Linearization and RNA synthesis: XmaI, T3 RNA concentration for injection: 100ng/μl
A293	pSP64T-*NUPL1-gfp-nos1*-3'UTR	GFP fused in 3' to zebrafish nucleoporin like 1 and nos1 3'UTR for specific expression in PGCs. NUPL1 GenBank accession number NM_213229. Primers: 5'AGATCTATGTCTAGCTTTAACTTCGGCACAA3' 5'AGATCTGGCTCTCTTGCCCCTCTTGT3' Linearization and RNA synthesis: Not1 and Sp6 RNA concentration for injection: 100ng/μl
A528	pSP64T-*gfp-NUP155-nos1*-3'UTR	GFP fused in 5' to zebrafish nucleoporin 155 and nos1 3'UTR for specific expression of GFP in PGCs. NUP155 GenBank accession number NM_200156. Primers: 5'GGATCCATGCCGTCCAGTCTGGGCTC3' RNA concentration for injection: 100ng/μl 5'GGATCCTCAGTGCAGCTTCTCCAGCT3' Linearization and RNA synthesis: Not1 and Sp6
A532	pSP64T-*gfp-kinesin11-nos1*-3'UTR	GFP fused in 5' to zebrafish kinesin11 and nos1 3'UTR for specific expression in PGCs. Kinesin11 GenBank accession number NM_173261. Primers: 5'GGATCCATGGCATCATCACAAGTACCAGC3' 5'GGATCCACCACCTCTCTACTCCTCGG3' Linearization and RNA synthesis: Not1 and Sp6 RNA concentration for injection: 100ng/μl

A545	pSP64T-*gfp-dyneinlike2-nos1*-3'UTR	GFP fused in 5' to Dynein light chain 2 like nos1 3'UTR for specific expression of GFP in PGCs. Genebank accession number NM_001030000 Primers: 5'AGATCTATGACTGACAGGAAGGC3' 5'AGATCTTCAGCCCGATTTAAAG3' Linearization and RNA synthesis: Not1 and Sp6 RNA concentration for injection: 100ng/μl
A623	pSP64T-*dynamitin-nos1*-3'UTR	Dynactin subunit P50 dynamitin fused to nos1 3'UTR for specific expression of GFP in PGCs. Overexpression disrupts normal dynein function. Genebank accession number DQ141218 Primers: 5'GGATCCATGGCCGACCCGAAGTACG3' 5'CTCGAGCTACTTGTTGAGTTTCTTCATCCTCTG3' Linearization and RNA synthesis: Not1 and Sp6 RNA concentration for injection: 100ng/μl

Other plasmids used in this work		
Plasmid No.	**Name**	**Description**
344	pSP64T-*H1M-gfp-nos1-3'UTR*	Zebrafish Histone 1 protein fused to GFP and nos1 3'UTR for specific expression of GFP in the PGCs.
355	pSP6-GFP-nos1 3'UTR	GFP fused to nos1 3'UTR for specific expression of GFP in PGCs.
493	pSP64 EGFP-F-nos1 3'UTR	Expression of farnesylated EGFP to label membrane of germ cells, localized by the nos1 3'UTR
509	pSP64 N19RhoA-nos1 3'UTR	Dominant negative RhoA. Mutation T19N. Fused to nos1 3'UTR for specific expression of GFP in PGCs.
534	pSP64	Vasa N-terminal region fused to GFP and nos1 3'UTR

	vasaGFP-nos1 3'UTR	for specific expression of GFP in PGCs.
779	pSP64T-*clip170-gfp-nos1*-3'UTR	Microtubule binding protein Clip170 fused to GFP and nos1 3'UTR for specific expression in PGCs.

4.6 Equipment

Cameras	- RT slider Spot, Diagnostic Instruments
	-RT SE Spot, Diagnostic Instruments
	- Leica DC 300, Leica
Injector	- PV830 Pneumatic PicoPump, World
	- Precision Instruments (USA)
Needle puller	- PN-30 Microelectrode Puller, Science Products
PCR machines	- Cyclone 96, Peqlab, Erlangen
	- Mastercycler Personal, Eppendorf
Microscopes	- Zeiss Axioplan 2, Zeiss
	- Leica confocal microscope TCS SL
Centrifuges	Eppendorf 5415D, Eppendorf
Spectrophotometer	Eppendorf 6131, Eppendorf

4.7 Programs, Database,

Image processing	Adobe Photoshop 7.0, Adobe, ImageJ
Microscopy	- Metamorph, Universal Imaging Corp.
	- Leica confocal software, Leica
Multiple sequence alignment	Sequencher, Gene Codes Corp.
Cloning	Vector NTI, Invitrogen (USA) www.zfin.org,

	www.sanger.ac.uk/Projects
Office application	Microsoft
Literature	PubMed www.ncbi.nln.nih.gov,
Databases	- Endnote 8.0, Thomson
	- FileMaker Pro 7, FileMaker Inc.
BLAST-programs	- bl2seq www.ncbi.nlm.nih.gov
	- blastn
	- blastp
	- tblastn
Multiple sequence alignment	clustalW
	www2.ebi.ac.uk/clustalw

4.8 Molecular Biology

4.8.1 Plasmid DNA Isolation from E. coli

E. coli containing a certain plasmid were inoculated into 5 ml (Miniprep), 50 ml (Midiprep) LB Standard Medium (1% Bacto-Tryptone (Gibco BRL), 0.5% Bacto-Yeast Extract (Gibco BRL), 1% NaCl in Millipore water) with 50 μg/ml ampicillin or kanamycin, and incubated at 37 °C shaking for 16 hours. The plasmid was extracted using Plasmid Mini, Midi or Maxi Kit (Qiagen) according to the manufacturer instruction, eluted in milipore water and the concentration was measured using a BioPhotometer (Eppendorf).

For transcription, the Mini/Midi DNA was further purified by extraction with 1 volume of phenol/chloroform/ isoamylalcohol (25:24:1) once or twice, followed by 13,500 rpm centrifugation for 10 minutes. The supernatant was carefully collected and subjected twice to 1 volume of chloroform, again followed by centrifugation and supernatant collection. Then, the DNA was precipitated with 0.1 volume of 3 M NaAc, pH 5.2 and 2.5 volume of ethanol 100 % on ice for 30 min or for low amounts of DNA at –20 °C for 15 minutes. Afterwards, the DNA was pelleted by centrifugation at 13,500 rpm and 4 °C for 15 minutes, washed with 1 ml 70% ethanol, centrifuged at 13,500 rpm for another 5 minutes, air dried, and dissolved in a proper volume of Millipore H_2O.

4.8.2 DNA and RNA Electrophoresis and Purification from Agarose Gel

0.5-2% agarose gel was prepared by melting agarose (Biozym) in 1×TAE Buffer (400 mM Tris, 0.2M Acetic acid, 10 mM EDTA, pH 8.0) and subsequently adding ethidium bromide to a final concentration of 0.3 μg/ml. DNA and RNA sample were mixed with 5×DNA Loading Buffer (25% Ficoll, 100 mM EDTA, 0.05% Bromophenol Blue), and electrophoresis was performed under 1-7 V/cm in 1×TAE buffer.

For DNA isolation, the DNA band was cut from the gel and DNA was isolated using the UltraCleanTM 15 DNA Purification Kit (MO BIO) or the QIAquick Gel extraction Kit as described by the manufacturers.

4.8.3 DNA Digestion with Restriction Enzymes

For DNA analysis, about 50-200ng DNA was digested with 3-10 U restriction enzymes at the appropriate temperature for 45-60 minutes. For DNA preparation, 1-10 μg DNA was incubated with 20-40 U restriction enzymes at the appropriate temperature for at least 4 hours.

4.8.4 Dephosphorylating and Blunting of DNA Fragment

5'-ends of DNA fragment dephosphorylation was performed by directly adding 1 μl Alkaline Phophatase (1U/μl, Roche) into the restriction enzyme digestion mixture and incubating at 37 °C for 1 hour.

DNA polymerase I large fragment (Klenow fragment) (5U/μl, NEB) was used to fill-in the ends of 5'-overhang DNA fragment. DNA in restriction enzyme NEBuffer supplemented with 33 μM dNTPs was incubated with Klenow at a concentration of 1 U per μg DNA at 25 °C for 30 minutes.

3'-overhang DNA fragment was blunted using T4 DNA Polymerase (5U/μl, Roche) in the restriction enzyme NEBuffer supplemented with 50 μM dNTPs.

4.8.5 Ligation

25-100 ng purified vector fragment was mixed with 3-10 folds (molecular ratio) of purified insert fragment, 1 μl 10× T4 DNA ligase buffer (MBI Fermentas), and 1 μl T4 DNA ligase (3 U/μl, MBI Fermentas) in a total volume of 10 μl. This ligation mixture was incubated at RT for at least 2 hours or overnight at 16 °C.

Alternatively, insert of e.g. PCR fragments were cloned by TOPO cloning according to the standard protocol of the Topo-TA Cloning Kit (Invitrogen) and PCR II, PCR 2.1 and PCR 4 vectors were used.

4.8.6 Standard PCRs

For standard PCR, primers were designed with 15-24 nucleotides and a melting temperature (TM) between 50 °C and 68 °C. The reaction mixture contains 1 µl template cDNA (10pg-100ng cDNA), 2.5 µl of forward primer (5mM), 2.5 µl of reverse primer (5mM), 2.5 µl 10× Amersham PCR Buffer, 2.5 µl 2.5 mM dNTPs, and 1 µl Tag Polymerase (5U/µl) in a total volume of 25 µl. The thermocycling program (Table) was carried out as described below.

Step	Temperature	Duration
1. Initial Denaturation	92 °C	1 minute
2. Denaturation	92 °C	15 seconds
3. Annealing	T_M – 4 °C	20 seconds
4. Annealing and Elongation	72 °C	1 minute/kb
5. Go to Step 2, 15-30 cycles		
6. Final Elongation	72 °C	3-15 minutes

Table 4: The thermocycling program for standard PCR.

4.8.7 High Fidelity PCRs

The Advantage HF 2 PCR Kit (Clontech) was used for high fidelity PCR and PCRs starting from low amount of template DNA according to manufactures instruction.

4.8.8 Preparation of Electrocompetent E. coli Cells and Transformation by Electroporation

Preparation of electrocompetent *E.coli* cells was performed as described below.

1. Inoculate two single colonies of *E. coli* into 2×10 ml LB medium and cultured at 37 °C shaking overnight (250 rpm).
2. Inoculate the 2×10 ml overnight cultures into 2×1 liter prewarmed LB medium and culture them at 37 °C shaking until the $O.D._{600}$ reached 0.6-0.8 (about 3 hours).
3. Chill the cells on ice for 10-30 minutes.
4. Centrifuge at 5,000 rpm at 4 °C for 20 minutes to harvest the cells.
5. Discard the supernatant, wash each pellet from 1 liter culture with 1 liter prechilled water (1:1 wash), then centrifuge at 5,000 rpm at 4 °C for 20 minutes.
6. Discard the supernatant, wash each pellet with 100 ml prechilled 10% glycerol (1:10 wash), then centrifuge at 6,000 rpm (Sorvall HS-4 rotor) at 4 °C for 10 minutes.
7. Discard the supernatant, wash each pellet with 20 ml prechilled 10% glycerol (1:50 wash), then centrifuge at 6,000 rpm at 4 °C for 10 minutes.
8. Discard the supernatant, wash each pellet with 2 ml prechilled 10% glycerol (1:500 wash), then centrifuge at 6,000 rpm at 4 °C for 5 minutes.
9. Aspirate the supernatant, resuspend each pellet in 2-3 ml 10% glycerol. 40 µl or 80 µl resuspension was aliquoted into each tube on ice, frozen in liquid nitrogen, and stored at –80 °C.

Table 5: Preparation of electrocompetent *E. coli* cells.

50 µl competent cells were thawed on ice and transferred into a prechilled 0.1 cm electrode Gene Pulser Cuvette (Bio-Rad). 1-5 µl DNA solution (1-100 ng/µl) or 1-5 µl ligation product was added directly into the competent cells and mixed well by gently flicking. Then, the surface of the cuvette was completely dried and the electroporation was performed using Gene Pulser (Bio-Rad) under the condition of 1.8 kV, 200 Ω resistance, 25 µF capacitance. Afterwards, 960 µl prewarmed LB medium was immediately supplied to the electroporated *E. coli* for recovery. The cells were recovered at 37 °C rotating for 1 hour, followed by plating 100 µl and 900 µl on separate selective plates.

4.8.9 Sequencing of DNA plasmids

Plasmids used in this work where sequenced by SeqLab Goettingen, Germany and MWG Ebersberg, Germany.

4.9 Zebrafish

4.9.1 Fish breeding and incubation

Zebrafish were raised and kept under standard laboratory conditions at a constant light-dark cycle (14 h light/10 h dark [107],[108]. For breeding, 2 fish were placed in a mating tank, separated by a net over night. In the following morning, the separating net was removed that zebrafish could lay. To avoid parental cannibalism the cage separated parents from eggs. The eggs were collected and transferred to methylene blue egg water or Danieau's solution to prevent the growth of fungi or bacteria. The eggs were maintained at 28.5 °C until the desired stages. Alternatively, to accelerate or slow down the development, embryos were incubated at 30 °C or 25 °C, respectively.

Morphological features were used to determine the stage of the embryo according to Kimmel at al.,1995.

30x Danieau's stock solution	**for 1 liter**
1.74M NaCl (M=58.44 g/mol)	101.7 g
21mM KCl (M=74.56 g/mol)	1.57 g
12mM MgSO4[7H2O] (M=246.48 g/mol)	2.96 g
18mM Ca(NO3)2[4H2O)] (M=236.15 g/mol)	4.25 g
150mM HEPES (M=238.31 g/mol)	35.75 g
pH 7.6	
0.3x Danieau's solution = working solution	
1:100 dilution of stock and pH adjustment with a view drop of 5M NaOH to pH 7.6	
5 ml Penicilin and Streptomycin (100x stock solution – 10'000U/ml, Gibco) / 1 liter of Danieau's may added to suppress bacterial growth.	

Table 6: Danieau solution

4.9.2 Linearization of Plasmid for in vitro transcription

5-10 μg plasmid DNA was linearized by incubating with 2-4 μl restriction enzyme at 37 °C for 4 hours, purified with PCR Purification Kit (Qiagen), and eluted in 30 μl H2O. 1 μl elution was loaded on an agarose gel to check the linearization efficiency.

4.9.3 mRNA Synthesis for Injection

Synthesis of 7-methyl-guanosine capped sense mRNA for injections was produced according to the standard protocol of mMESSAGE mMACHINE Kit (Ambion) (see in table below)

1. 1 μl 10x Reaction buffer, 5 μl 2x Nucleotide Mix / Cap analog, 50-500ng linearized DNA template, 0.8 μl T3, T7 or SP6 Enzyme Mix, H2O to a final volume of 10 μl were mixed and incubated for 2h at 37° C.
2. To degrade DNA, 0,5 μl DNAseI were added and incubate for 20 min at 37 °C.
Phenol-Chloroform extraction
3. Add 260 μl DEPC water
4. Add 30 μl Ammonium Acetate Stop Solution (Message Machine Kit) and mix
5. Add 300 l PCI (= Phenol-Chloroform-Isoamylalcohol, 25: 24 : 1, „for RNA“, pH=6,6, from Ambion)
6. Shake vigorously (or vortex) 10 seconds; spin 15 minutes at RT; carefully transfer upper phase to a new tube. Do not take interphase – discard lower phase.
7. Add CI (= Chloroform-Isoamylalcohol, 24:1), shake vigorously, spin 7 minutes, transfer supernatant to new tube.
8. repeat CI step once.
Precipitation and Analysis
9. Add equal volume of 100% Isopropanol (room temp.). Do not incubate at –20°C as recommended by the Ambion kit.
10. Centrifuge immediately, 40 minutes. Don’t precool the centrifuge, cool

down to 4°C while spinning.
11. Carefully remove the supernatant using a pipette.
12. Wash 2x with 80% EtOH (RT)
13. After second wash, remove large drops using a pipette; air dry for a minimum time
14. Dissolve in 20 µl HEPES (10mM, pH 7,4, DEPC water). Pipette up and down to dissolve.
The amount and the quality of the obtained RNAs were estimated by gel electrophoresis and measurements of the UV absorption at λ 260/280nm.

Table 7: Synthesis of sense mRNA for injection of zebrafish embryos.

4.9.4 Injection of Zebrafish Embryos

mRNA was diluted with HEPES (10mM, pH 7,4, DEPC water) at different concentration. After fertilized zebrafish eggs were collected, aligned in a 1.5 % agarose ramp, about 2-4 nl RNA solution was injected into each yolk of the embryo. Post-microinjection embryos were kept at 28.5 °C in Danieau's medium and were checked several hours later to remove the unfertilized and dead eggs.

4.9.5 Immunostaining of Zebrafish Embryos

Immunostaining of zebrafish embryos was performed as described below.

1. Embryos were fixed in methanol 100% for 2h at RT
2. Wash PBTB (PBS pH 7.4, 0.1% Tween-20, 0.2% Triton X-100, 1% BSA) for 3h at RT on shaker.
3. Primary antibody: rabbit-anti vasa (1:1500; P2), anti-HA (1:200; P4) dissolved in PBTB o/n at 4 °C.
4. Wash PBTX (PBS pH 7.4, 0.1% Tween-20, 0.2% Triton X-100) for 7h at RT on shaker, in total 12 changes
5. Secondary antibody: goat-anti-mouse 488 (1:200) and goat-anti-rabbit 546 (1:200) in PBTB overnight at 4 °C
6. Wash PBTX for 7h at RT on shaker, in total 12 changes

7. Store at 4 °C for microscopy.

Table 8: Immunostaining protocol.

4.9.6 DIG- Labeled RNA Probe Synthesis

DIG- labeled antisense RNA probes were synthesized by incuabting 1 μg – 100ng linearized DNA, 4 μl 5×Transcription Buffer (Fermentas), 2 μl DIG-Labeling Mixture (Roche), 1 μl RNAse inhibitor, 2 μl SP6, T3 or T7 RNA Polymerase (Fermentas, Roche) in a total volume of 20 μl at 37 °C for 2-2.5 hours. To degrade DNA, 0,5 μl DNAseI (Fermentas) were added and incubate for 20 min at 37 °C.

For RNA probe precipitation, 11μl NH_4Ac 7,8M (=1/2 Vol) and 63 μl ethanol 100 % RT (= 3 Vol) were added, mixed and let precipitate for 30-50 minutes at RT. Following, precipitate were collected by spinning 30-40 minutes at maximum speed at 20 °C and washed once with 1 ml ethanol 80 % RT. Air dried pellet was dissolved in 20 μl H_2O and 80 μl Hyb-buffer (see below).

Alternative to RNA probe precipitation, the transcription product was supplemented with 30 μl H_2O, purified with a G-50 Sephadex Micro Columns according to manufactures instruction and 80 μl Hyb-buffer added to the elut. 3 μl purified probe was checked on an agarose gel.

4.9.7 Zebrafish One-Colour Whole Mount In Situ Hybridization

Zebrafish embryos were fixed in 4% PFA/PBS at 4 °C overnight, embryos younger than 2 somite stage were fixed for 2 days. Fish were twice washed with PBS 8 g/l NaCl, 0.2 g/l KCl, 1.8 g Na_2HPO_4 *2 H_2O, 0.24 g KH_2PO_4, pH 7,2) or PBT (PBS, 0.1 % Tween 20), dechorionated after fixation until the 16-somite stage. Later stages were dechorionated prior to fixation, using forceps and up to 50 embryos per 1.5 ml tube were subjected to whole-mount *in situ* hybridization (Table).

	Treatment and Solution	T	Duration
Dehydration	1. 5x methanol 100%	RT	5 minutes
The embryos in 100% methanol can be stored in –20 °C for several months.			
1. Day	1. 75% methanol/PBT, shaking.	RT	5 minutes
	2. 50% methanol/PBS, shaking.	RT	5 minutes
	3. 25% methanol/PBT, shaking.	RT	5 minutes
	4. Wash 4x PBT	RT	5 minutes each
	5. Digest with 5 µg/ml Proteinase K (1:1000 dilution from stock in PBT).	RT	< bud : no 1 somite : 30 sec 5 somite : 1-3 min 24 hpf : 3 – 5 min
	6. Wash 3x PBT	RT	1 minutes each
	7. Refixation with 4% PFA in PBS	RT	20 minutes
	8. Wash 5x PBT	RT	5 minutes each
	9. Prehybridize in prewarmed Hyb buffer (50% formamide, 5×SSC, 9mM Citric acid monohydrate to pH 6.0 – 6.5, 0.1% Tween 20, 500 µg/ml PCI extracted Torula yeast tRNA (SIGMA), 50 µg/ml heparin), incubated in a waterbath. [20x SSC; 3M NaCl, 0.3 M Na_3Citrat]	67 °C	2 -5 hours
	10. Dilute 1:200 to 5:200 Dig labeled RNA probe into Hyb-buffer. Hybridize with 200 µl Hyb-buffer per 1.5 ml tube of this solution	67 °C	Overnight
	1. Wash with Hyb buffer	67 °C	20 min

2. Day	2. Wash 3x with 50% SSCT 2x/50% Formamide	67 °C	20 min
	3. Wash 1x with 75% SSCT 2x/25% Formamide	67 °C	20 min
	4. Wash 2x with SSCT 2x	67 °C	20 min
	5. Wash 4x with SSCT 0.2x	67 °C	30 min
	6. Wash 1x with PBT	67 °C	5 min
	7. Blocking with Blocking solution (5% sheep serum and 10 mg/ml BSA in PBT)	RT	1 to several hours
	8. Antibody Incubation 1 with 200 µl preabsorbed Antibody solution: 1:2000 Anti-Dig (Roche), 2% sheep serum and 2 mg/ml BSA in PBT	4 °C	Overnight
3. Day	1. Wash 3x with PBT;	RT	5 minutes
	2. Wash 8x with PBT	RT	Within 3 hours
	3. Wash 3x with NTMT (100 mM Tris HCl pH 9.5, 50 mM $MgCl_2$, 100 mM NaCl, 0.3% Tween 20) for 20 ml use: 2ml Tris HCl pH 9.5, 1M / 1ml $MgCl_2$, 1M / 2ml NaCl, 1M / 600 µl Tween 20, 10% / 14.8 ml H_20	RT	5 minutes each
	4. Transfer embryo into a 24 well plate, using a cut 1 ml pipet tip		
	5. Staining (blue): remove most NTMT and add 0.5 ml staining solution (1 ml NTMT, 4.5 µl NBT -	37 °C	Various

	Nitro Blue Tetrazolium, Sigma N6876, 75 mg/ml in 70% DMF / 30% H2O), 3.5 µl X-phosphate (=BCIP, 50 mg/ml in 100% DMF) to each well.		
	6. Stop reaction by removing staining solution and wash 2x with PBT and (only for one colour *in situ* hybridization experiment) 3x with Stop solution (1mM EDTA, 0.1% Tween, 0.05M phosphate buffer pH 5.8 [for 200ml: 92ml 0.1M NaH2PO4, 8ml 0.1M Na2HPO4 - this mixture produce a pH of 5.8])	RT	5 min each
Transfer embryos in 80% Glycerol / 20% Stop solution.			

Table9: Whole-mount *in situ* hybridization of zebrafish embryos.

4.10 Microscopy and Time-Lapse Analysis

Bright field and fluorescence pictures were made with a Zeiss Axioplan 2 microscope or a Leica confocal DMRXE microscope.

For the time-lapse analysis embryos were oriented in agarose ramps overlaid with 0.3x Danieau's solution. Time-lapse movies were generated using Metamorph software (Universal Imaging) controlling a Zeiss Axioplan2 microscope.

4.10.1 Fluorescent live imaging

4.10.1.1 Epifluorescence microscopy

Images were obtained using a Zeiss Axioplan2 microscope controlled by the Metamorph software (Universal Imaging). High magnification time-lapse movies were generated using a 63x or 40x objective capturing frames at 10

second intervals. 3D reconstructions where done using the Metamorph software (Universal Imaging).

4.10.1.2 Confocal-Microscopy

Images were obtained using a Leica TCS Confocal microscope controlled by the internal Leica software. High magnification time-lapse movies were generated using a 63x objective capturing frames 10 or 15-second intervals. Pictures were recorded in the xyzt modus (allows z-stacks as well as recordings over time) with 512x512 or 1024x1024 pixel resolution. The laser intensity, potentiometer, gain and offset were adjusted according to the individual conditions of the experiments (fluorescent intensity based on the probe characteristics).

4.11 Nocodazole treatment

Nocodazole (CALBIOCHEM) stock solution of 10mg/ml was prepared in DMSO and used at a concentration of 10μg/ml or 1μg/ml. Embryos were injected with mRNA generated from the constructs pSP64T-*vasa-dsRedEx,* pSP64T-*H1M-gfp-nos1-3'UTR* and pSP64T-*clip170-gfp-nos1*-3'UTR, and grown for 11 hours. They were decorionated and either recorded after 4 hours of exposure to the drug, or pictures where taken after exposure over night. *In vivo* epifluorescence microscopy movies where done while embryos where exposed to the drug.

4.12 Bleaching experiments and intensity measurements

Embryos where injected in one cell stage with *vasa-GFP-nos3'UTR* RNA. The larger granule within one germ cell was selected using the ROI command of Leica confocal software. Granules where exposed to 4 bleaching periods of 1 minute each. GFP fluorescent pictures of Vasa-GFP expressing granules were taken every 5 minutes and fluorescence intensity was measured using ImageJ software. Measurements of plasma membrane intensity within the same cell where taken in order to control possible variations of laser intensity. Data documentation was done by using the Microsoft Excel program.

Intensity measurements of DynL2-GFP a dividing germ cell was done by using the imageJ software.

4.13 Granules number and granule size calculations

Total number of granules was calculated using 3D reconstructions of confocal stack series of germ cells labelled for Vasa protein. 3D reconstructions where made using the imageJ software, and granules where counted directly from each image.

Granule area calculations where done by measuring length and width of each granule using the internal Leica software. The average of these values represented the total granule diameter. The granule radio was obtained using the formula D= 2r (D=diameter, r=radio). Area was calculated by Area=πr^2. Data processing and statistical analyses were done by using the Microsoft Excel program.

5.0 Summary

5.1 Structural characterization of zebrafish germ plasm of primordial germ cells

In zebrafish, germ cells are responsible for transmitting the genetic information from one generation to the next. During the first cleavages of zebrafish embryonic development, a specialized part of the cytoplasm known as germ plasm, is responsible of committing four blastomeres to become the progenitors of all germ cells in the forming embryo.

Much is known about how the germ plasm is spatially distributed in early stages of primordial germ cell development, a process described to be dependant on microtubules and actin. However, little is known about how the material is inherited after it reorganizes into a perinuclear location, or how is the symmetrical distribution regulated in order to ensure proper inheritance of the material by both daughter cells. It is also not clear whether there is a controlled mechanism that regulates the number of granules inherited by the daughter cells, or whether it is a random process.

We describe the distribution of germ plasm material from 4hpf to 24hpf in zebrafish primordial germ cells using Vasa protein as marker. Vasa positive material appears to be conglomerate into 3 to 4 big spherical structures at 4hpf. While development progresses, these big structures become smaller perinuclear granules that reach a total number of approximately 30 at 24hpf. We investigated how this transformation occurs and how the minus-end microtubule dependent motor protein Dynein plays a role in this process. Additionally, we describe specific colocalization of microtubules and perinuclear granules during interphase and more interestingly, during all different stages of cell division. We show that distribution of granules follow what seems to be a regulated distribution: during cells division, daughter cells inherit an equal number of granules. We propose that due to the permanent colocalization of microtubular structures with germinal granules during interphase and cell division, a coordinated mechanism between these structures may ensure proper distribution of the material among daughter cells. Furthermore, we show that exposure to the microtubule-depolymerizing

drug nocodazole leads to disassembly of the germ cell nuclear lamin matrix, chromatin condensation, and fusion of granules to a big conglomerate, revealing dependence of granular distribution on microtubules and proper nuclear structure.

6.0 Zusammenfassung

6.1 Strukturelle Charakterisierung des Keimplasmas primordialer Keimzellen im Zebrafisch

Keimzellen sichern als Vorläuferzellen von Eizelle und Spermium die Weitergabe der genetischen Information von einer Generation zur Nächsten. Während der ersten Zellteilungen der frühen Embryogenese werden vier Blastomere durch die Aufnahme eines spezialisierten Teils des Zytoplasmas, dem Keimplasma, als Vorläuferzellen aller Keimzellen des sich entwickelnden Embryos festgelegt.

Die asymmetrische Vererbung des Keimplasmas in der frühen embryonalen Entwicklung ist gut untersucht und wird durch Mikrotubuli und Aktin gesteuert. Die Vererbung des Keimplasmas nach der perinukleären Reorganisation und die Mechanismen, die die korrekte Verteilung auf beide Tochterzellen sicherstellen, sind jedoch weitestgehend unerforscht.

In dieser Arbeit wird die Verteilung des Keimplasmas in der Zeit der symmetrischen Zellteilung von 4 Stunden bis 24 Stunden nach der Befruchtung anhand des Keimplasmamarkers Vasa beschrieben. 4 Stunden nach der Eibefruchtung sammelt sich Vasa-positives Material in drei bis vier großen, sphärischen Granula an, die sich im Laufe der ersten 24 Stunden zu etwa 30 kleineren perinukleären Granulae aufteilen. Wir untersuchen die Kolokalisation von Mikrotubuli und perinukleären Granula in allen Zellzyklusstadien und zeigen dass Mikrotubuli und deren Motorproteine die Struktur und Reorganisation von Granulae ermöglichen. Weiterhin scheint die Vererbung der Granulae einer geregelten Verteilung zu unterliegen, da eine gleiche Anzahl an Granula auf beide Tochterzellen während der Mitose verteilt wird. Analog zu der Reorganisation des Keimplasmas in kleinere Strukturen wird für die symmetrische Vererbung ein Mikrotubuli-abhängiger Mechanismus vorgeschlagen, der eine korrekte Verteilung des Keimplasmas auf beide Tochterzellen sicherstellt. Die Beobachtungen verdeutlichen, dass im Zebrafisch die Verteilung von Keimplasma in primordialen Keimzellen von Mikrotubuli und einer intakten Struktur des Zellkerns abhängig ist.

7.0 References

1. Raz, E., and Reichman-Fried, M. (2006). Attraction rules: germ cell migration in zebrafish. Curr Opin Genet Dev *16*, 355-359.
2. Kunwar, P.S., Siekhaus, D.E., and Lehmann, R. (2006). In vivo migration: a germ cell perspective. Annu Rev Cell Dev Biol *22*, 237-265.
3. Xie, T., and Spradling, A.C. (2000). A niche maintaining germ line stem cells in the Drosophila ovary. Science *290*, 328-330.
4. Nieuwkoop, P.D., and Sutasurya, L.A. (1976). Embryological evidence for a possible polyphyletic origin of the recent amphibians. J Embryol Exp Morphol *35*, 159-167.
5. McLaren, A. (1999). Signaling for germ cells. Genes Dev *13*, 373-376.
6. Wylie, C. (2000). Germ cells. Curr Opin Genet Dev *10*, 410-413.
7. Seydoux, G., and Strome, S. (1999). Launching the germline in Caenorhabditis elegans: regulation of gene expression in early germ cells. Development *126*, 3275-3283.
8. Knaut, H., Pelegri, F., Bohmann, K., Schwarz, H., and Nusslein-Volhard, C. (2000). Zebrafish vasa RNA but not its protein is a component of the germ plasm and segregates asymmetrically before germline specification. J Cell Biol *149*, 875-888.
9. Mahowald, A.P. (1968). Polar granules of Drosophila. II. Ultrastructural changes during early embryogenesis. J Exp Zool *167*, 237-261.
10. Eddy, E. (1975). Germ plasm and the differentiation of the germ cell line. Int. Rev. Cytol. *43*, 229-280.
11. Williamson, A., and Lehmann, R. (1996). Germ cell development in Drosophila. Annu Rev Cell Dev Biol *12*, 365-391.
12. Seydoux, G., and Fire, A. (1994). Soma-germline asymmetry in the distributions of embryonic RNAs in Caenorhabditis elegans. Development *120*, 2823-2834.
13. Knaut, H., Pelegri, F., Bohmann, K., Schwarz, H., and Nusslein-Volhard, C. (2000). Zebrafish vasa RNA but not its protein is a component of the germ plasm and segregates asymmetrically before germline specification. J Cell Biol *149*, 875-888.
14. Hashimoto, Y., Maegawa, S., Nagai, T., Yamaha, E., Suzuki, H., Yasuda, K., and Inoue, K. (2004). Localized maternal factors are required for zebrafish germ cell formation. Dev Biol *268*, 152-161.
15. Illmensee, K., and Mahowald, A.P. (1974). Transplantation of posterior polar plasm in Drosophila. Induction of germ cells at the anterior pole of the egg. Proc Natl Acad Sci U S A *71*, 1016-1020.
16. Weidinger, G., Stebler, J., Slanchev, K., Dumstrei, K., Wise, C., Lovell-Badge, R., Thisse, C., Thisse, B., and Raz, E. (2003). *dead end*, a novel vertebrate germ plasm component, is required for zebrafish primordial germ cell migration and survival. Current Biology *13*, 1429-1434.
17. Köprunner, M., Thisse, C., Thisse, B., and Raz, E. (2001). A zebrafish nanos-related gene is essential for the development of primordial germ cells. Genes Dev *15*, 2877-2885.
18. Schupbach, T., and Wieschaus, E. (1986). Maternal-effect mutations altering the anterior-posterir pattern of the Drosophila embryo. Roux's Arch.Dev. Biol. *195*, 302-317.
19. Abdelhaleem, M. (2005). RNA helicases: regulators of differentiation. Clin Biochem *38*, 499-503.

20. Styhler, S., Nakamura, A., Swan, A., Suter, B., and Lasko, P. (1998). vasa is required for GURKEN accumulation in the oocyte, and is involved in oocyte differentiation and germline cyst development. Development *125*, 1569-1578.
21. Lasko, P., and Ashburner, M. (1988). The product of the Drosophila gene vasa is very similar to eukaryotic initiation factor-4A. Nature *335*, 611-617.
22. Hay, B., Jan, L., and Jan, Y. (1988). A protein component of Drosophila polar granules is encoded by vasa and has extensive sequence similarity to ATP-dependent helicases. Cell *55*, 577-587.
23. Gavis, E.R., Lunsford, L., Bergsten, S.E., and Lehmann, R. (1996). A conserved 90 nucleotide element mediates translational repression of nanos RNA. Development *122*, 2791-2800.
24. Shibata, N., Umesono, Y., Orii, H., Sakurai, T., Watanabe, K., and Agata, K. (1999). Expression of vasa(vas)-related genes in germline cells and totipotent somatic stem cells of planarians. Dev Biol *206*, 73-87.
25. Braat, A., Zandbergen, T., van de Water, S., Goos, H., and Zivkovic, D. (1999). Characterization of zebrafish primordial germ cells: morphology and early distribution of vasa RNA. Dev Dyn *216*, 153-167.
26. Yoon, C., Kawakami, K., and Hopkins, N. (1997). Zebrafish vasa homologue RNA is localized to the cleavage planes of 2- and 4-cell-stage embryos and is expressed in the primordial germ cells. Development *124*, 3157-3165.
27. Pelegri, F., Knaut, H., Maischein, H., Schulte-Merker, S., and Nusslein-Volhard, C. (1999). A mutation in the zebrafish maternal-effect gene nebel affects furrow formation and vasa RNA localization. Curr Biol *9*, 1431-1440.
28. Pelegri, F. (2003). Maternal factors in zebrafish development. Dev Dyn *228*, 535-554.
29. Theusch, E.V., Brown, K.J., and Pelegri, F. (2006). Separate pathways of RNA recruitment lead to the compartmentalization of the zebrafish germ plasm. Dev Biol *292*, 129-141.
30. Braat, A.K., Speksnijder, J.E., and Zivkovic, D. (1999). Germ line development in fishes. Int J Dev Biol *43(7*, 745-760.
31. Forbes, A., and Lehmann, R. (1998). Nanos and Pumilio have critical roles in the development and function of Drosophila germline stem cells. Development *125*, 679-690.
32. Deshpande, G., Calhoun, G., Yanowitz, J.L., and Schedl, P.D. (1999). Novel functions of nanos in downregulating mitosis and transcription during the development of the Drosophila germline. Cell *99*, 271-281.
33. Gavis, E.R., and Lehmann, R. (1994). Translational regulation of nanos by RNA localization. Nature *369*, 315-318.
34. Bashirullah, A., Halsell, S., Cooperstock, R., Kloc, M., Karaiskakis, A., Fisher, W., Fu, W., Hamilton, J., Etkin, L., and Lipshitz, H. (1999). Joint action of two RNA degradation pathways controls the timing of maternal transcript elimination at the midblastula transition in Drosophila melanogaster. EMBO Journal *18*, 2610-2620.
35. Mishima, Y., Giraldez, A.J., Takeda, Y., Fujiwara, T., Sakamoto, H., Schier, A.F., and Inoue, K. (2006). Differential regulation of germline mRNAs in soma and germ cells by zebrafish miR-430. Curr Biol *16*, 2135-2142.
36. Whitington, P.M., and Dixon, K.E. (1975). Quantitative studies of germ plasm and germ cells during early embryogenesis of Xenopus laevis. J Embryol Exp Morphol *33*, 57-74.
37. Boswell, R.E., and Mahowald, A.P. (1985). tudor, a gene required for assembly of the germ plasm in Drosophila melanogaster. Cell *43*, 97-104.
38. Thomson, T., and Lasko, P. (2005). Tudor and its domains: germ cell

formation from a Tudor perspective. Cell Res *15*, 281-291.
39. Mogilner, A., Wollman, R., Civelekoglu-Scholey, G., and Scholey, J. (2006). Modeling mitosis. Trends Cell Biol *16*, 88-96.
40. Malmanche, N., Maia, A., and Sunkel, C.E. (2006). The spindle assembly checkpoint: preventing chromosome mis-segregation during mitosis and meiosis. FEBS Lett *580*, 2888-2895.
41. King, S.M. (2000). The dynein microtubule motor. Biochim Biophys Acta *1496*, 60-75.
42. Hayden, J.H., Bowser, S.S., and Rieder, C.L. (1990). Kinetochores capture astral microtubules during chromosome attachment to the mitotic spindle: direct visualization in live newt lung cells. J Cell Biol *111*, 1039-1045.
43. Holy, T.E., and Leibler, S. (1994). Dynamic instability of microtubules as an efficient way to search in space. Proc Natl Acad Sci U S A *91*, 5682-5685.
44. Coue, M., Lombillo, V.A., and McIntosh, J.R. (1991). Microtubule depolymerization promotes particle and chromosome movement in vitro. J Cell Biol *112*, 1165-1175.
45. Cassimeris, L. (2004). Cell division: eg'ing on microtubule flux. Curr Biol *14*, R1000-1002.
46. Welte, M.A. (2004). Bidirectional transport along microtubules. Curr Biol *14*, R525-537.
47. Endow, S.A., and Barker, D.S. (2003). Processive and nonprocessive models of kinesin movement. Annu Rev Physiol *65*, 161-175.
48. Paschal, B.M., and Vallee, R.B. (1987). Retrograde transport by the microtubule-associated protein MAP 1C. Nature *330*, 181-183.
49. Bullock, S.L., and Ish-Horowicz, D. (2001). Conserved signals and machinery for RNA transport in Drosophila oogenesis and embryogenesis. Nature *414*, 611-616.
50. Holzbaur, E.L., and Vallee, R.B. (1994). DYNEINS: molecular structure and cellular function. Annu Rev Cell Biol *10*, 339-372.
51. Johnson, K.A., and Wall, J.S. (1983). Structure and molecular weight of the dynein ATPase. J Cell Biol *96*, 669-678.
52. Vallee, R.B., Wall, J.S., Paschal, B.M., and Shpetner, H.S. (1988). Microtubule-associated protein 1C from brain is a two-headed cytosolic dynein. Nature *332*, 561-563.
53. Gill, S.R., Schroer, T.A., Szilak, I., Steuer, E.R., Sheetz, M.P., and Cleveland, D.W. (1991). Dynactin, a conserved, ubiquitously expressed component of an activator of vesicle motility mediated by cytoplasmic dynein. J Cell Biol *115*, 1639-1650.
54. Boylan, K., Serr, M., and Hays, T. (2000). A molecular genetic analysis of the interaction between the cytoplasmic dynein intermediate chain and the glued (dynactin) complex. Mol Biol Cell *11*, 3791-3803.
55. Karki, S., and Holzbaur, E.L. (1999). Cytoplasmic dynein and dynactin in cell division and intracellular transport. Curr Opin Cell Biol *11*, 45-53.
56. Burkhardt, J.K., Echeverri, C.J., Nilsson, T., and Vallee, R.B. (1997). Overexpression of the dynamitin (p50) subunit of the dynactin complex disrupts dynein-dependent maintenance of membrane organelle distribution. J Cell Biol *139*, 469-484.
57. Goshima, G., Nedelec, F., and Vale, R.D. (2005). Mechanisms for focusing mitotic spindle poles by minus end-directed motor proteins. J Cell Biol *171*, 229-240.
58. Nedelec, F.J., Surrey, T., Maggs, A.C., and Leibler, S. (1997). Self-organization of microtubules and motors. Nature *389*, 305-308.

59. Sharp, D.J., Rogers, G.C., and Scholey, J.M. (2000). Microtubule motors in mitosis. Nature *407*, 41-47.
60. Vale, R.D. (2003). The molecular motor toolbox for intracellular transport. Cell *112*, 467-480.
61. Burke, B., and Ellenberg, J. (2002). Remodelling the walls of the nucleus. Nat Rev Mol Cell Biol *3*, 487-497.
62. Herrmann, H., and Aebi, U. (2000). Intermediate filaments and their associates: multi-talented structural elements specifying cytoarchitecture and cytodynamics. Curr Opin Cell Biol *12*, 79-90.
63. Lopez-Soler, R.I., Moir, R.D., Spann, T.P., Stick, R., and Goldman, R.D. (2001). A role for nuclear lamins in nuclear envelope assembly. J Cell Biol *154*, 61-70.
64. Moir, R.D., Spann, T.P., Herrmann, H., and Goldman, R.D. (2000). Disruption of nuclear lamin organization blocks the elongation phase of DNA replication. J Cell Biol *149*, 1179-1192.
65. Hutchison, C.J. (2002). Lamins: building blocks or regulators of gene expression? Nat Rev Mol Cell Biol *3*, 848-858.
66. Gruenbaum, Y., Margalit, A., Goldman, R.D., Shumaker, D.K., and Wilson, K.L. (2005). The nuclear lamina comes of age. Nat Rev Mol Cell Biol *6*, 21-31.
67. Fahrenkrog, B., and Aebi, U. (2003). The nuclear pore complex: nucleocytoplasmic transport and beyond. Nat Rev Mol Cell Biol *4*, 757-766.
68. Tran, E.J., and Wente, S.R. (2006). Dynamic nuclear pore complexes: life on the edge. Cell *125*, 1041-1053.
69. Aaronson, R.P., and Blobel, G. (1974). On the attachment of the nuclear pore complex. J Cell Biol *62*, 746-754.
70. Stutz, F., and Izaurralde, E. (2003). The interplay of nuclear mRNP assembly, mRNA surveillance and export. Trends Cell Biol *13*, 319-327.
71. Weirich, C.S., Erzberger, J.P., Flick, J.S., Berger, J.M., Thorner, J., and Weis, K. (2006). Activation of the DExD/H-box protein Dbp5 by the nuclear-pore protein Gle1 and its coactivator InsP6 is required for mRNA export. Nat Cell Biol *8*, 668-676.
72. Zeligs, J.D., and Wollman, S.H. (1979). Mitosis in rat thyroid epithelial cells in vivo. IV. Cell surface changes. J Ultrastruct Res *67*, 297-308.
73. Drummond, S., Ferrigno, P., Lyon, C., Murphy, J., Goldberg, M., Allen, T., Smythe, C., and Hutchison, C.J. (1999). Temporal differences in the appearance of NEP-B78 and an LBR-like protein during Xenopus nuclear envelope reassembly reflect the ordered recruitment of functionally discrete vesicle types. J Cell Biol *144*, 225-240.
74. Margalit, A., Vlcek, S., Gruenbaum, Y., and Foisner, R. (2005). Breaking and making of the nuclear envelope. J Cell Biochem *95*, 454-465.
75. Ellenberg, J., Siggia, E.D., Moreira, J.E., Smith, C.L., Presley, J.F., Worman, H.J., and Lippincott-Schwartz, J. (1997). Nuclear membrane dynamics and reassembly in living cells: targeting of an inner nuclear membrane protein in interphase and mitosis. J Cell Biol *138*, 1193-1206.
76. Yang, L., Guan, T., and Gerace, L. (1997). Integral membrane proteins of the nuclear envelope are dispersed throughout the endoplasmic reticulum during mitosis. J Cell Biol *137*, 1199-1210.
77. Nurse, P. (1990). Universal control mechanism regulating onset of M-phase. Nature *344*, 503-508.
78. Collas, P. (1999). Sequential PKC- and Cdc2-mediated phosphorylation events elicit zebrafish nuclear envelope disassembly. J Cell Sci *112 (Pt 6)*,

977-987.
79. Macaulay, C., Meier, E., and Forbes, D.J. (1995). Differential mitotic phosphorylation of proteins of the nuclear pore complex. J Biol Chem *270*, 254-262.
80. Favreau, C., Worman, H.J., Wozniak, R.W., Frappier, T., and Courvalin, J.C. (1996). Cell cycle-dependent phosphorylation of nucleoporins and nuclear pore membrane protein Gp210. Biochemistry *35*, 8035-8044.
81. Joseph, J., Liu, S.T., Jablonski, S.A., Yen, T.J., and Dasso, M. (2004). The RanGAP1-RanBP2 complex is essential for microtubule-kinetochore interactions in vivo. Curr Biol *14*, 611-617.
82. Zeligs, J.D., and Wollman, S.H. (1979). Mitosis in rat thyroid epithelial cells in vivo. I. Ultrastructural changes in cytoplasmic organelles during the mitotic cycle. J Ultrastruct Res *66*, 53-77.
83. Maul, G.G. (1977). Nuclear pore complexes. Elimination and reconstruction during mitosis. J Cell Biol *74*, 492-500.
84. Duesberg, P., Li, R., Fabarius, A., and Hehlmann, R. (2005). The chromosomal basis of cancer. Cell Oncol *27*, 293-318.
85. Du, Y., Ferro-Novick, S., and Novick, P. (2004). Dynamics and inheritance of the endoplasmic reticulum. J Cell Sci *117*, 2871-2878.
86. Birky, C.W., Jr. (1983). Relaxed cellular controls and organelle heredity. Science *222*, 468-475.
87. Birky, C.W., Jr. (1983). The partitioning of cytoplasmic organelles at cell division. Int Rev Cytol Suppl *15*, 49-89.
88. Warren, G., and Wickner, W. (1996). Organelle inheritance. Cell *84*, 395-400.
89. Maniotis, A., and Schliwa, M. (1991). Microsurgical removal of centrosomes blocks cell reproduction and centriole generation in BSC-1 cells. Cell *67*, 495-504.
90. Wilson, E.B. (1916). The Distribution of the Chondriosomes to the Spermatozoa in Scorpions. Proc Natl Acad Sci U S A *2*, 321-324.
91. Kloc, M., and Etkin, L.D. (2005). RNA localization mechanisms in oocytes. J Cell Sci *118*, 269-282.
92. Shima, D.T., Cabrera-Poch, N., Pepperkok, R., and Warren, G. (1998). An ordered inheritance strategy for the Golgi apparatus: visualization of mitotic disassembly reveals a role for the mitotic spindle. J Cell Biol *141*, 955-966.
93. Madaule, P., Eda, M., Watanabe, N., Fujisawa, K., Matsuoka, T., Bito, H., Ishizaki, T., and Narumiya, S. (1998). Role of citron kinase as a target of the small GTPase Rho in cytokinesis. Nature *394*, 491-494.
94. Kosako, H., Yoshida, T., Matsumura, F., Ishizaki, T., Narumiya, S., and Inagaki, M. (2000). Rho-kinase/ROCK is involved in cytokinesis through the phosphorylation of myosin light chain and not ezrin/radixin/moesin proteins at the cleavage furrow. Oncogene *19*, 6059-6064.
95. Scholey, J.M., Rogers, G.C., and Sharp, D.J. (2001). Mitosis, microtubules, and the matrix. J Cell Biol *154*, 261-266.
96. Echeverri, C.J., Paschal, B.M., Vaughan, K.T., and Vallee, R.B. (1996). Molecular characterization of the 50-kD subunit of dynactin reveals function for the complex in chromosome alignment and spindle organization during mitosis. J Cell Biol *132*, 617-633.
97. Ressom, R.E., and Dixon, K.E. (1988). Relocation and reorganization of germ plasm in Xenopus embryos after fertilization. Development *103*, 507-518.
98. Solecki, D.J., Govek, E.E., and Hatten, M.E. (2006). mPar6 alpha controls neuronal migration. J Neurosci *26*, 10624-10625.
99. Warren, G. (1993). Membrane partitioning during cell division. Annu Rev

Biochem *62*, 323-348.
100. Shorter, J., and Warren, G. (2002). Golgi architecture and inheritance. Annu Rev Cell Dev Biol *18*, 379-420.
101. Colanzi, A., Suetterlin, C., and Malhotra, V. (2003). Cell-cycle-specific Golgi fragmentation: how and why? Curr Opin Cell Biol *15*, 462-467.
102. Berekelya, L.A., Mikryukov, A.A., Luchinskaya, N.N., Ponomarev, M.B., Woodland, H.R., and Belyavsky, A.V. (2007). The protein encoded by the germ plasm RNA Germes associates with dynein light chains and functions in Xenopus germline development. Differentiation.
103. Arkov, A.L., Wang, J.Y., Ramos, A., and Lehmann, R. (2006). The role of Tudor domains in germline development and polar granule architecture. Development *133*, 4053-4062.
104. Chuma, S., Hosokawa, M., Kitamura, K., Kasai, S., Fujioka, M., Hiyoshi, M., Takamune, K., Noce, T., and Nakatsuji, N. (2006). Tdrd1/Mtr-1, a tudor-related gene, is essential for male germ-cell differentiation and nuage/germinal granule formation in mice. Proc Natl Acad Sci U S A *103*, 15894-15899.
105. Pitt, J., Schisa, J., and Priess, J. (2000). P granules in the germ cells of Caenorhabditis elegans adults are associated with clusters of nuclear pores and contain RNA. Dev Biol *219*, 315-333.
106. Sengoku, T., Nureki, O., Nakamura, A., Kobayashi, S., and Yokoyama, S. (2006). Structural basis for RNA unwinding by the DEAD-box protein Drosophila Vasa. Cell *125*, 287-300.
107. Kimmel, C., Ballard, W., SR, K., B, U., and TF, S. (1995). Stages of embryonic development of the zebrafish. Developmental Dynamics *203*, 253-310.
108. Westerfield, M. (1995). The Zebrafish Book (Oregon: University of Oregon Press).

8.0 Acknowledgments

I am grateful to the eternal support of my family in whatever I do, right or wrong. I want to thank my sister Michelle for her dedication and unconditional support, and for her eternal trust on me. I want to thank my father for his aura of happiness that surrounds me even when he is far. For his wisdom and deep love that he shares with me. I am thankful to my mother for being the fundamental pillar of my life. I thank them all three for making my hard decisions easier. I am thankful to David for his unconditional help and generosity, and for giving me the most beautiful nephew. I thank Lucas for lightning my days.

I want to thank my supervisor Erez Raz for giving me the opportunity of reaching a higher scientific level that I am sure, will be fundamental for my next professional steps. I specially want to thank Bijan and Markus for their fundamental opinions and corrections on the text and for their sweet friendship. Without them, it would have been more difficult to complete this manuscript. I want to thank Juerg for his fundamental support and discussion on a project that we started together. I will be eternally thankful to Sonia and Elena for being my close friends during these years. I will carry them both deep in my heart to wherever I go. I want also to thank Heiko for his useful comments and discussion on my work, and Michal for her great generosity and predisposition to help. Special thanks for Julia, Helene and Ursula for their invaluable technical support. I am grateful to Iad and Markus for collaborating with my in this work.
I will be forever grateful to science and its humanity.

9.0 Appendix

9.1 Affidavit

Hiermit versichere ich, dass ich die vorliegende Dissertation selbständig und ohne unerlaubte Hilfe angefertigt und andere als die in der Dissertation angegebenen Hilfsmittel nicht benutzt habe. Alle Stellen, die wörtlich oder sinngemäß aus veröffentlichten oder unveröffentlichten Schriften entnommen sind, habe ich als solche kenntlich gemacht. Kein Teil dieser Arbeit ist in einem anderen Promotions- oder Habilitationsverfahren verwendet worden.

Here I declare that my thesis entitled “Structural characterization and distribution of zebrafish germ plasm during interphase and mitosis” has been done independently and with no other sources and aids than quoted and listed below.

Figure 6c: Cloning and Time-lapse analysis of NUP155 where done in collaboration with La-lad Nakkrasae.

Figure 7a: Picture of Nucleoporin immunostaining was done by Juerg Stebler.

Figure 9a, b: Pictures of α-Tubulin immunostaining were done by Juerg Stebler.

Figure 16a: Transgenic was generated by Markus Strasser. Pictures where done in collaboration.

Figure 18 : Cloning of Kinesin11 and Dynein ligh chain 2 like where done in collaboration with La-lad Nakkrasae.

Kassel, 23 April 2007 your signature